Agricultural Water Management 294 (2024) 108696

Contents lists available at ScienceDirect

Agricultural Water Management

journal homepage: www.elsevier.com/locate/agwat

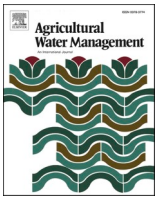

Localizing agricultural impacts of 21st century climate pathways in data scarce catchments: A case study of the Nyando catchment, Kenya

Katoria Lekarkar [a,*], Albert Nkwasa [b,a], Lorenzo Villani [c,a], Ann van Griensven [a,d]

[a] Department of Water and Climate, Vrije Universiteit Brussel (VUB), 1050 Brussels, Belgium
[b] International Institute for Applied Systems Analysis (IIASA), Schlossplatz 1, A-2361 Laxenburg, Austria
[c] Department of Agriculture, Food, Environment and Forestry, University of Florence, Italy
[d] Water Science & Engineering Department, IHE Delft Institute for Water Education, 2611 AX Delft, the Netherlands

ARTICLE INFO

Handling Editor-Dr Z Xiying

Keywords:
Climate change
Agriculture
Crop water use
Crop yields
Sub-Saharan Africa
SWAT+

ABSTRACT

Climate change is projected to increase the volatility of agricultural productivity within the Sub-Saharan Africa region. However, current knowledge of climate change impacts in this region is largely derived from coarse-grid global datasets that lack sufficient detail for local applications. The derived impacts are thus generalized across large spatial scales, with a limited representation the differential exposure across the region. It is thus necessary to conduct localized assessments to derive local vulnerabilities and develop context-specific mitigation strategies. This study utilizes downscaled outputs from regional climate models to quantify the effects of climate change on maize and sugarcane crops at catchment-scale, hereby the Nyando catchment in Kenya. The findings indicate that climate change will reduce the suitability of conditions to the growth of both crops, with sub-optimal conditions for maize increasing by up to 600%. The analysis of crop yields show that maize yields are projected to decline by about 23.9% under the RCP4.5 scenario and 29.4% under RCP8.5. Sugarcane yields are similarly projected to decrease by 17.0% and 28.6% for RCP4.5 and RCP8.5 respectively. The underlying climatic changes suggest that future warming outweighs the effects of precipitation in explaining crop yield declines. More broadly, the methodology applied in this study can be readily adapted and utilized for agricultural areas throughout the Sub-Saharan region. By adopting this localized impact assessment approach policymakers and sector players will be empowered with information at a higher spatial detail which empowers targeted, region-specific adaptation strategies.

1. Introduction

Climate change is conceivably one of the most pressing challenges of the 21st century, having far-reaching and detrimental consequences across various sectors (Mitchell et al., 2006; Patz et al., 2014). The IPCC Sixth Assessment Report (AR6) observes that global warming has accelerated over recent years and projects that global temperatures will continue to increase under all emission scenarios unless emissions of greenhouse gases are drastically reduced. Several studies e.g. Adhikari et al. (2015), IPCC (2022), Jia et al. (2022) have shown that climate change has a considerable impact on global water circulation as a warmer climate will intensify the hydrological cycle and increase the variability of precipitation and water availability. These alterations have profound implications on the agricultural sector, which accounts for 70% of all global water uses and 92% of all freshwater consumed globally (Liu and Yang, 2010; Chaturvedi et al., 2015) as well as broader implications on food security and allocation of water resources for multiple uses (Siebert et al., 2010; Jia et al., 2022; Tian et al., 2023).

The complex and interconnected impacts of climate change pose significant challenges to agricultural systems worldwide. Climate change projected to disproportionately affect agriculture in Sub-Saharan Africa (SSA), with widespread impacts amplified by low productivity, limited institutional and financial capacity but more so by a high reliance on rainfed agriculture, in which at least 90–95% of all croplands is rainfed (Cook and Vizy, 2013; Sultan and Gaetani, 2016; Abrams, 2018; Woetzel et al., 2020). Since 1961, agricultural productivity in SSA has shrunk by 26–34% due to climate change, exceeding changes in all other regions globally (Ortiz-Bobea et al., 2021). The volatility of agricultural productivity is expected to worsen further as precipitation patterns shift and conditions become unfavorable for crops, many of which are

* Corresponding author.
E-mail address: katoria.lesaalon.lekarkar@vub.be (K. Lekarkar).

https://doi.org/10.1016/j.agwat.2024.108696
Received 15 September 2023; Received in revised form 31 December 2023; Accepted 19 January 2024
Available online 14 February 2024

already at the physical threshold beyond which productivity will start to decline (Woetzel et al., 2020). Projections indicate that crop yields in the region are expected to decline by about 10% under a 2˚C warming, with more adverse impacts at higher warming, to the extent that some areas will be rendered unsuitable for crop production (Burke et al., 2009; Schaeffer et al., 2013).

Due to sparse and intermittent in situ climate observations in many parts of SSA, studies of climate change effects on crop yields in the region have conventionally been conducted at continental and regional scales (e.g. Thornton et al., 2009; Tatsumi et al., 2011; Washington and Pearce, 2012; Waithaka et al., 2013; Adhikari et al., 2015; Nkwasa et al., 2023). While providing valuable insights and broad generalizability in the magnitude and direction of impacts, much of these studies are conducted by directly applying rather coarse resolution (>50 km) climate outputs from global and regional climate models (GCMs and RCMs) and other global datasets e.g. soils at similar resolution. This poses a number of important limitations. Foremost, GCM and RCM data can exhibit biases in representing historical climate patterns and can thus add a layer of uncertainty when used to drive impact models (Sultan and Gaetani, 2016). In addition, the scale of such datasets is spatially aggregated and thus loses the relevant variation in physico-climatic conditions that exist at local scales (e.g.mountainous regions) and also conflicts with the spatial scale at which farm-scale operations are implemented. Coarse grid-scale GCM and RCM data also operate at scales larger than the local influence of factors, such soil properties and the partitioning of rainfall into runoff, evapotranspiration and storage, which affect crop growth locally (Baron et al., 2005; Sultan and Gaetani, 2016; Müller et al., 2021). As Trisos et al. (2022) postulates, the impacts derived from the application of such coarse-scale datasets lack the statistical power to disaggregate the differential vulnerability and exposure that exists over various parts of Africa. In a study covering the Sahelian belt, Baron et al. (2005) demonstrate that spatial aggregation significantly influences the characteristics of seasonal rainfall. This, in turn, led to an overestimation of grain yields and crop biomass by up to 40% when this aggregated data was used to drive a crop model. Mearns et al. (2001), while investigating the effect of varying soil input resolution into a process-based crop model, similarly found that aggregating soil input parameters significantly affected the spatial variance and pattern of maize and soybean yields. Consistently, Waha et al. (2015), in a study of some maize growing areas of Burkina Faso, find that the spatial resolution of different soil, climate and management information affects simulated yields across crop models. Although the authors argue that using the most detailed input datasets does not necessarily increase the robustness of crop yield simulations, they suggest that the appropriateness of input data and model choice should take precedence in a modelling study.

As climate policies increasingly emphasize adaptation, conducting localized assessments of climate change impacts in SSA becomes imperative for contextualizing local-scale dynamics and identifying vulnerabilities. Such insights are crucial for developing robust, context-specific adaptation strategies that safeguard the resilience and sustainability of agricultural practices and food security against climate-related shocks. Achieving this goal necessitates climate change studies that offer detailed information at a higher spatial resolution. While the scarcity and access to in situ climate data still remains a persistent challenge across SSA, various hybrid climate datasets that morph remotely sensed (satellite) data with station observations to produce consistent, long-term climate variables (> 30 years) have now become widely available. These datasets are available at spatial resolutions higher than RCMs and GCMs and their representation of different climatic conditions has been validated quasi-globally (see for instance Funk et al., 2015; Maidment et al., 2017; Verdin et al., 2020; Beck et al., 2022). The availability of these datasets offers opportunities to downscaling outputs from RCMs and GCMs which enables the assessment of climate change impacts at localized scales and deriving impacts that are relevant to local stakeholders.

The goal of this study is thus to leverage on these datasets to downscale climate data from RCMs and subsequently explore the influence of climate change on crop yields in a typical agriculture-dominated, data-scarce SSA catchment. We also extend the study to include the assessment of crop water use, which has remained largely understudied despite it being an important input for food production. Herein, we apply the analysis to the Nyando Catchment in Kenya where agriculture is the dominant land use and consumer of water. The assessment is based on a simulation approach using the improved process-based Soil and Water Assessment Tool Plus (SWAT+) to investigate the impacts of rising temperatures, atmospheric carbon dioxide, and precipitation variations on individual crop water consumption and yields for two major crops - maize and sugarcane - which hold significant socio-economic value in the region. In as far as is practically possible, the study uses open-access datasets and well elaborated workflows which are applicable to similar geographical domains.

2. Materials and methods

2.1. Overview of the study area

Nyando catchment is located within the Lake Victoria Basin, covering an estimated area of 3550 km^2. Geographically, the catchment extends between latitudes 0.43˚S and 0.10˚ N and longitudes 34.5˚E and 35.7˚E. (Olang et al., 2014; Ouma et al., 2020). The drainage has an east-west orientation, originating from the western scarps of the Kenyan Rift Valley at an altitude of about 3000 m and draining into the Winam Gulf of Lake Victoria at about 1170 m above sea level, as shown in Fig. 1. Annual rainfall is characterized by a bimodal pattern with the dominant long rainy season occurring over March-May and the short rains lasting from September to December (Mutua et al., 2020).

The catchment lies within two major Koppen-Geiger climate zones. At the eastern forested highland headwaters, the catchment experiences a temperate climate with annual rainfall of up to 1800 mm (Fig. 2). The western half of the catchment experiences a warmer tropical climate with less distinct dry and wet seasons with annual rainfall typically varying between 600 and 1100 mm. (Peel et al., 2007; Opere and Okello, 2011; Beck et al., 2018). Annual mean temperature in the catchment remains fairly constant, fluctuating between a mean maximum of 25˚C and a mean minimum about 12˚C.

Land use is predominantly rainfed mixed subsistence agriculture, which occupies more than 60% of the catchment and where seasonal crops like maize, beans, and sorghum are the most common (Fig. 3). Subsistence agriculture is oriented with the seasonal pattern of rainfall within the catchment (Gathenya et al., 2011; Salat and Swallow, 2018), with crops cultivated over the two rainy seasons. The start of the first cropping season coincides with the onset of the long rains, extending from March to July while the second cycle lasts through the duration of the short rains (Place et al., 2006; Swallow et al., 2008). Large-scale commercial sugarcane farming occupies the middle areas of the catchment while commercial tea production is concentrated on the high potential foot slopes of the catchment.

2.2. Model description

In this study the SWAT+ model was used due to its capability to represent complex interacting ecosystem and hydrological processes and simulating the impacts of climate change on both micro and macro-scales. SWAT is a physically based, time-continuous, catchment-scale model which has been extensively utilized to assess the impacts of climate and land management practices on water resources over different time scales. The model has been widely applied to quantify agricultural water withdrawals (Schuol et al., 2008; Jeyrani et al., 2021) and to simulate crop yields across a wide range of spatial scales ranging from field scales (Sinnathamby et al., 2017), catchment scales (Chen et al., 2019; Musyoka et al., 2021) to continental scales (Abbaspour

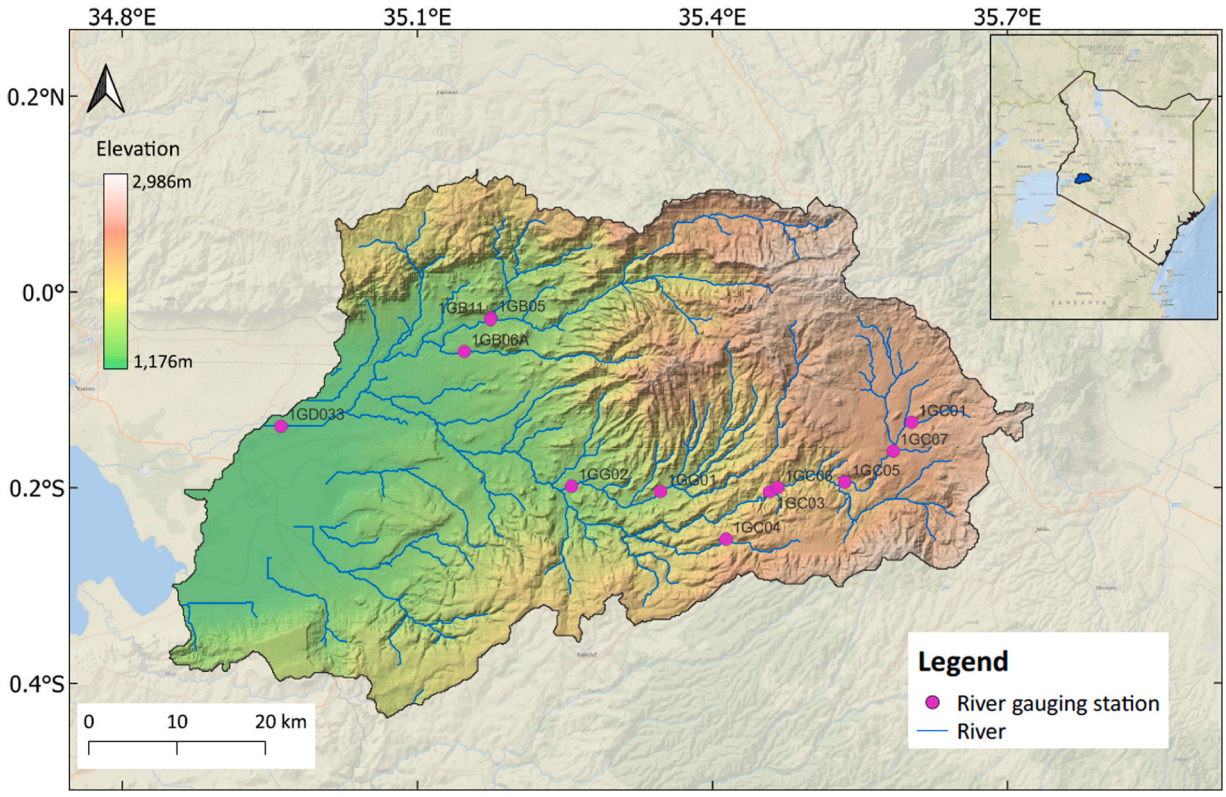

Fig. 1. Topography and drainage of the Nyando Catchment.

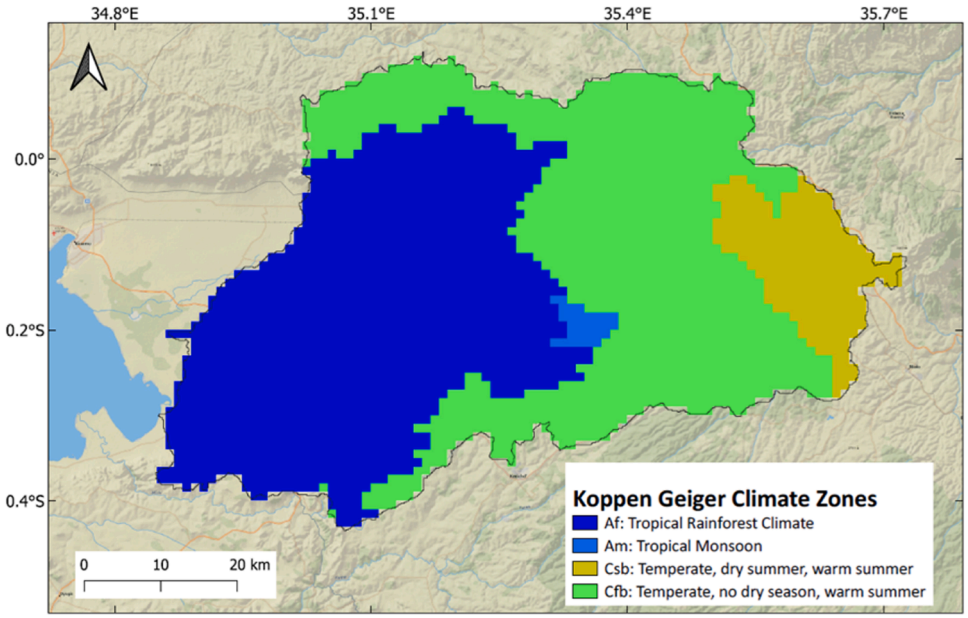

Fig. 2. Köppen-Geiger Climate zones of the Nyando catchment.

et al., 2015). The model has undergone significant improvements to its latest version, SWAT+. These include an enhanced flexibility to discretize and configure watersheds and represent interactions and processes within a watershed. The model computes water balance components at the hydrologic response units (HRUs)- catchment units with unique land use, topography, soil types and management conditions. SWAT+ also introduces new algorithms to implement complex rule-based management actions through the use of decision tables for land management and reservoir operations. This allows SWAT+ to execute decision-based farm operations-such as the timing of planting, fertilizer application, the timing and amount of irrigation- more robustly and realistically (Bieger et al., 2017).

Plant growth in the model is based on the Erosion Productivity Impact Calculator (EPIC), a mathematical cropping systems model which incorporates various physical components that include weather simulation, crop growth, soil-erosion and sedimentation, nutrient cycling and crop management practices (Stockle et al., 1992; Mearns et al., 2001; Neitsch et al., 2009). Crop growth in SWAT+ can be

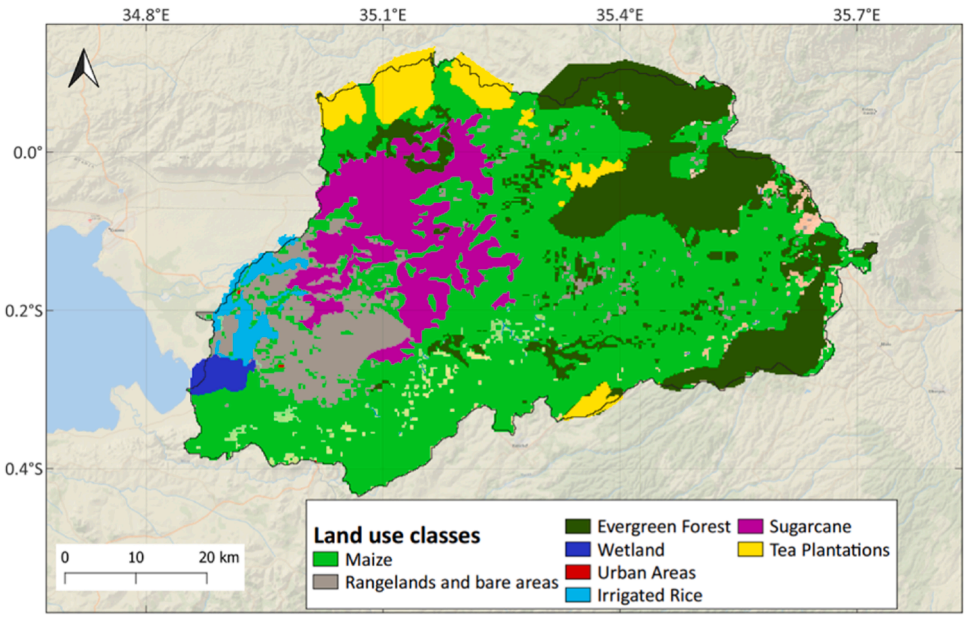

Fig. 3. Major land use classes in Nyando Catchment.

scheduled according to calendar dates or the daily accumulated plant heat units and is modelled by simulating leaf area development and interception of light which is subsequently transformed into plant biomass using a plant-specific radiation use efficiency, the amount of dry biomass per unit of intercepted radiation (Stockle et al., 1992). If the planting and harvesting dates are not specified, the model simulates the growth period of annual crops until the heat units accumulate to reach the crop potential heat units. For perennial crops, growth begins from when the base temperature of the plant is exceeded and continues throughout the year, with the plants maintaining their root system during the entire period of growth (Williams et al., 1989). Actual growth can be inhibited by extreme temperatures and water and nutrient stresses (Neitsch et al., 2009). Crop yields in the model are calculated using a fraction of the above-ground dry plant biomass at the time of harvest, known as the harvest index. For a given day of the crop growth cycle, the model calculates the harvest index as;

$$HI = HI_{opt} \cdot \frac{100 \cdot f_{PHU}}{(100 \cdot f_{PHU} + \exp[11.1 - 10 \cdot f_{PHU}])} \quad (1)$$

Where; HI = harvest index, HI_{opt} = potential harvest index at plant maturity under ideal growing conditions and f_{PHU} = fraction of accumulated plant heat units.

The crop yield is then computed from the harvest index as:

$$yield = \begin{cases} bio_{ag} \cdot HI & \text{if } HI \leq 1.00 \\ \text{bio} \cdot \left(1 - \frac{1}{(1 + HI)}\right) & \text{if } HI > 1.00 \end{cases} \quad (2)$$

Where; *yield* is the crop yield in kg/ha, bio_{ag} represents the total above-ground biomass on the day of harvest (kg/ha) and *bio* is the total plant biomass on the day of harvest (kg/ha).

For climate change studies, the dependency of plant biomass on atmospheric CO_2 concentration is simulated by integrating a CO_2 concentration value into the computation of radiation-use efficiency, as expressed by the relationship: (Neitsch et al., 2009);

$$RUE = \frac{100 \cdot CO_2}{CO_2 + \exp(r_1 - r_2 \cdot CO_2)} \quad (3)$$

Where; RUE = Radiation-use efficiency (kg/ha.(MJ/m^2))$^{-1}$, r_1 and r_2 are shape coefficients.

SWAT+ can simulate plant evapotranspiration using two methods, the Penman-Monteith and the Priestly-Taylor methods. However, only through the Penman-Monteith method can the effects of atmospheric CO_2 concentration on crop water use be modelled. The Penman-Monteith equation (Allen et al., 1998) is given by:

$$\lambda ET = \frac{\Delta(R_n - G) + \rho_a \cdot C_p \cdot \frac{(e_s - e_a)}{r_a}}{\Delta + \gamma \cdot \left(1 + \frac{r_c}{r_a}\right)} \quad (4)$$

λ = Latent heat of vaporization (MJ/kg), ET = Evaporation (kg/m^2/day), R_n = Net radiation at the crop surface (MJ/m^2/day), G = Soil heat flux density (MJ/m^2/day), ρ_a = Mean air density at constant pressure (kg/m^3), C_p = Specific heat capacity of air (MJ/kg/°C), e_s = Saturation vapor pressure (kPa), r_a = Actual vapor pressure (kPa), Δ = Slope of the saturation vapor pressure-temperature relationship (kPa/°C), γ = Psychrometric constant (kPa/°C), r_c = Canopy resistance (s/m), r_a = Aerodynamic resistance (s/m).

A comprehensive derivation of the aerodynamic and canopy resistance terms can be found in Stockle et al. (1992), Allen et al. (1998) and Neitsch et al. (2009) . Within SWAT+ , the canopy resistance is estimated by the ratio of the minimum surface resistance for a single leaf to one-half of the canopy leaf area index (Equation (5)).

$$r_c = \frac{r_l}{0.5 \cdot LAI} \quad (5)$$

Where r_c and r_l represent the canopy resistance and the maximum single leaf conductance (s/m) respectively while LAI represents the entire canopy leaf area index.

To simulate the effects of climate change on evapotranspiration, SWAT+ modifies the computation of leaf conductance to include a variable atmospheric CO_2 concentration value (Equation (6)).

$$C_{l,CO_2} = C_l \cdot \left[1.4 - 0.4 \cdot \frac{CO_2}{330}\right] \quad (6)$$

where C_{l,CO_2} is the leaf conductance (the inverse of leaf resistance) in (m/s) adjusted for CO_2 concentration and CO_2 represents the atmospheric concentration of carbon dioxide in ppmv.

Both equations are then merged to yield a single CO_2-adjusted canopy resistance term (Equation (7)) that is integrated into the Penman-Monteith equation.

$$r_c = r_l \cdot \left[\left(0.5 \cdot LAI \right) \cdot \left(1.4 - 0.4 \cdot \frac{CO_2}{330} \right) \right]^{-1} \quad (7)$$

The model further adjusts this canopy resistance term to account for the effect of high vapor pressure deficit on leaf conductance. The adjustment is based on a plant-specific threshold vapor pressure deficit, at which the leaf conductance of the plant begins to drop due to the vapor pressure deficit (Equation (8))

$$C_l = \begin{cases} C_{l,mx} \cdot (1 - \Delta C_{l,dcl}(vpd - vpd_{thr}) & \text{if } vpd > vpd_{thr} \\ C_{l,mx} & \text{if } vpd \leq vpd_{thr} \end{cases} \quad (8)$$

C_l is the single-leaf conductance (m/s), $C_{l,mx}$ is the maximum single-leaf conductance (m/s), $C_{l,dcl}$ represents the rate of decline of leaf conducatance per unit of vapor pressure deficit increase (m/s/kPa), *vpd* is the vapor pressure deficit (kPa) and vpd_{thr} is the threshold vapor pressure deficit (kPa).

2.2.1. Model input data

Meteorological input data required to drive the simulation in the SWAT+ model includes daily precipitation, minimum and maximum air temperature, solar radiation, relative humidity and wind speed. Due to the paucity of in situ data in Nyando catchment, the requisite simulation data was sourced from different sources. The input datasets were chosen through a comprehensive comparison of various gridded datasets using available in situ data and consulting literature evaluating the performance of gridded datasets. From this evaluation process, the following datasets were select as input to the model.

The Climate Hazards Infrared Precipitation with Stations (CHIRPS) dataset was selected for rainfall data. CHIRPS provides quasi-global rainfall data spanning latitudes 50°S–50°N at a resolution of 0.05° (approximately 5 km), and was developed to monitor extremes and evaluate precipitation-driven impacts (Funk et al., 2015). The dataset is available at daily, pentadal and monthly timescales from 1981 to present. It blends in situ data from Global Telecommunication System of the World Meteorological Organization with rainfall estimates derived from the calibration of global Cold Cloud Duration. Several studies have shown that CHIRPS exhibits a superior performance in tropical regions compared to other rainfall products (see e.g. (Maidment et al., 2017, Gebrechorkos et al., 2019, Msigwa et al., 2019). Gebrechorkos et al. (2019) report that CHIRPS adequately captures daily rainfall characteristics such as the total rainfall, total number of wet days and average amount of rainfall. Dinku et al. (2018), on a comparative analysis of different rainfall products over Eastern Africa, also found that CHIRPS shows a higher skill and low bias compared to the African Rainfall Climatology (ARC2) and the Tropical Applications of Meteorology using Satellite data (TAMSAT). Le and Pricope (2017), also showed that CHIRPS demonstrated a stronger temporal agreement with in situ data compared to the Climate Forecast System Reanalysis (CFSR) precipitation data. Consequently, CHIRPS has been used in several studies hydrological simulation studies (e.g. Tuo et al., 2016, Musie et al., 2019, Duan et al., 2019, Senent-Aparicio et al., 2021, Mengistu et al., 2022). Using data from several stations around the catchment, our assessment of the CHIRPS data also showed high correlation with in situ data (Pearson correlation values ranging from 0.77 to 0.91) and low bias on a monthly timescale (Supplementary material).

Temperature data was obtained from the Climate Hazards Center Infrared Temperature with Stations (CHIRTS-daily) (Funk et al., 2015). CHIRTS-daily is a product of merging monthly CHIRTS climate record, which combines temperature data from a global network of more than 15,000 stations and remotely sensed infrared land surface temperature, with daily temperature data from the fifth generation European Centre for Medium Range Weather Forecasts Reanalysis (ERA-5 2,3) (Verdin et al., 2020). The data covers the geographic extents 60°S–70°N with a 0.05° spatial resolution and is currently available from 1983 to 2016 (as of November 2023). Maximum and minimum daily temperatures are derived from anomalies and diurnal temperature range obtained from statistical downscaling of the ERA-5 data The resulting product exhibits a high correspondence with in situ data observations (daily correlations between 0.7 and 0.9) and also overcomes the significant cooling bias associated with ERA-5 data, which is most notable over Africa (Verdin et al., 2020).

Relative humidity, shortwave solar radiation and wind speed were obtained from the Multi-Source Weather (MSWX) data. MSWX is a global gridded near-surface meteorological derived from the fifth generation European Centre for Medium Weather Forecast reanalysis (ERA5), intended to improve the local accuracy and relevance of meteorological data for localized impact studies (Beck et al., 2022). MSWX-Past represents the historical portion of the record starting from January 1, 1979 to 5 days from real time. It is constructed by downscaling and bias correcting ERA5 0.28° reanalysis data using 0.1° resolution reference climatologies constructed from station observations, satellite imagery, and model outputs. The dataset offers some key competencies over other global meteorological products in that it has a high spatial (0.1^0) and temporal (3-hourly) resolution. The MSWX windspeed data is obtained by linearly interpolating ERA5 climatology on a monthly basis and subsequently rescaling the mean to match the 10-m wind speed from the Global Wind Atlas climatology. The short wave solar radiation is derived from a bilinear interpolation of ERA5 from which the long-term mean is rescaled to match that from the Global Solar Atlas. Since relative humidity is not a product of ERA5, the MSWX relative humidity is computed from the ERA5 dew point and air temperature (Beck et al., 2022). Land use categories were obtained from the European Space Agency Climate Change Initiative global land cover maps for the year 2015 (ESA, 2017) and reclassified according to the land use classes from Swallow et al. (2008). The digital elevation model for the catchment was extracted from the Shuttle Radar Topography Mission (SRTM) 90 m resolution DEM of Kenya (Farr et al., 2007, and soil classes were obtained from the digital Soil Map of the World developed by the Food and Agricultural Organization (FAO, 2003). Discharge data from the most downstream river gauging station of River Nyando were obtained from the Water Resources Authority of Kenya Table 1.

2.2.2. Model set up

The model was set up through the QSWAT+ interface in QGIS with the specified inputs of land use, DEM, soils, and climate data. To compute evapotranspiration, the Penman-Monteith method was selected on the basis that all required climate variables were available and since this is the only method with which the effect of increasing atmospheric CO_2 concentration- henceforth referred to as CO_2 fertilization can be accounted for in the model. The SCS curve number

Table 1
Overview of model input data and sources.

Dataset	Description	Sources
Topography	Digital Elevation Model (30 m)	The Shuttle Radar Topography Mission (Farr et al., 2007
Soils	1 km Digital Soil Map of the World	Food and Agricultural Organization (FAO, 2003
Land use	300 m climate Change Initiative land cover map	European Space Agency global Land Cover, Climate Change Initiative, version 2 (ESA, 2017) updated with catchment-specific land use classes from Swallow et al. (2008)
Climate	Daily precipitation, shortwave solar radiation, relative humidity, windspeed, minimum and maximum temperature	CHIRPS (Funk et al., 2015), CHIRTS-daily (Verdin et al., 2020), MSWX global bias-corrected meteorological data. (Beck et al., 2022
River Discharge	Daily river discharge data at station 1GD03	Water Resources Authority, Kenya

method was selected to simulate runoff while the variable storage method was adopted for routing flow. HRUs were created by lumping the catchment slopes into four slope bands of 0–5%, 5–15%, 15–25% and 25–40%, based on the analysis of the topography of the catchment. No threshold was set for HRUs so that all HRUs are included in the model simulation. The catchment was consequently delineated into 204 sub basins, 1078 landscape units and a total of 8559 HRUs were generated.

2.2.3. Implementing cropping patterns and management operations

In tropical regions, particularly in regions with alternating dry and wet seasons, crop cycles are dictated by moisture availability rather the accumulation of of plant heat units (Strauch and Volk, 2013; Alemayehu et al., 2017; Nkwasa et al., 2022). Our model set up thus defined crop growth and farm management operations using decision tables and management schedules that oriented planting with the availability of water. The cropping seasons in the study area were represented by scheduling farm operations according to information from field studies over the study area including (Mugalavai et al., 2013; Mulianga et al., 2015; Kipkulei et al., 2022) which report that planting is generally oriented with the occurrence of seasonal rainfall. The first cropping season of the maize crop was coincided with the onset of the long rains in March, continuing until harvest at the end of July with the second cropping season implemented between September and December. Planting was restricted only to periods when soil moisture reached 70% of field capacity, thereby avoiding planting during exceptionally dry periods and better simulating farmers' planting strategy. Sugarcane in the region has a cropping cycle of 18–24 months with planting predominantly during the rainy season. Harvesting is continuous throughout the year, based on the needs of the factories, crop maturity, rainfall and ratooning (Mulianga et al., 2015). To reflect these conditions, sugarcane in the model was planted when the threshold soil moisture level of 70% of field capacity was reached and harvested when the crop had accumulated sufficient heat units to reach maturity. Fertilizer was applied at the rate at 80 kg P ha^{-1} at planting and two split doses of 50 kg N ha^{-1} each at 3 and 6 months after planting, based on the recommendations of the Kenya Sugar Research Institute.

2.2.4. Simulation, calibration, and validation

To guarantee sufficient evaluation of model outputs, a baseline model was set up over the period 1981–2014, which overlaps with the period where observed data was available. Observed river flow data for hydrological calibration is intermittent, with availability limited to 1981–1989, 1991–1996 and 2005–2012. The model was first hydrologically calibrated using the SWAT+ Toolbox v1.0.1 (Chawanda, 2021), with 3-year warm-up period. Flow predictions were evaluated using three goodness of fit statistics namely; Nash-Sutcliffe Efficiency (NSE), percent bias (PBIAS) and root mean squared error (RMSE). Calibration of crop water use and crop yields was achieved by an iterative process of modifying decision tables and the plant growth characteristics database to optimize the representation of crop evapotranspiration (ET) patterns and crop yields. The average monthly ET for the respective crops were calibrated against ET data obtained from the Water Productivity through Open Access of Remotely sensed derived data version 2 (WaPOR v2.0) (FAO, 2020). WaPOR v2.0 is a database containing continuous actual evapotranspiration and interception (ETIa-WaPOR) data covering Africa and the Middle East available at three different resolutions, spanning from 2009 to date. The dataset provides the highest resolution of ET data available at the continental level (250 m), with a dekadal temporal resolution (FAO, 2020; Blatchford et al., 2020) and has been ranked as one of the best performing ET products over Africa, adequately capturing the magnitudes and spatial distribution of ET and presenting the least bias in long-term mean annual ET compared to other remote sensing ET products over the continent (Blatchford et al., 2020; Weerasinghe et al., 2020). For this study, the 250 m ET timeseries from WaPOR was extracted and spatially averaged over the HRUs for the respective crops and used to evaluate the simulated ET from the SWAT+ model on a monthly timescale, for the overlapping period 2009–2014. The model was hydrologically calibrated for the period 2005–2012 and validated between 1982–1988.

Areal weighted maize crop yields were obtained from the Food and Early Warning System Network database of crop production statistics (https://fews.net/) for the Western Kenya region while sugarcane yields were obtained from the FAOSTAT database (https://data.apps.fao.org/catalog/dataset/crop-production-yield-harvested-area-global-national-annual-faostat.

2.2.5. Assessing climate change impacts

Climate change impacts on the ET for the respective crops were derived by driving SWAT+ with projected meteorological outputs from five regional climate models (RCMs) from the Coordinated Regional Downscaling Experiment for the Africa domain (CORDEX-AFR-44), for two representative concentration pathways(RCPs)- RCP4.5 and RCP8.5 emission scenarios. The CORDEX-AFR-44 domain provides climate outputs at a spatial resolution of 0.44˚. The RCMs were chosen based on the availability of meteorological inputs required to drive the simulation in SWAT+ upon which the RCMs: KNMI-RACMO22T, CLMCom-CLM4–8-17, MPI-CSC-REMO2009, MIROC5-SMHI-RCA4 and MPI-M-MPI-ESM-LR-SMHI-RCA4 were selected. From each RCM, meteorological outputs were extracted for the baseline period 1981–2005 and the far future period 2076–2100. The input precipitation and temperature data for the baseline model was used to bias-correct RCM-derived precipitation and temperature using the multiplicative delta-change and the additive delta-change correction methods respectively (Graham et al., 2007; Teutschbein and Seibert, 2012). Subsequently the bias-corrected inputs were used to drive SWAT+ to obtain outputs for both historical and scenario periods, retaining the baseline model parameterization.

To account for CO_2 fertilization, ambient CO_2 concentrations of 370 ppmv, 533 ppmv and 827 ppmv were prescribed respectively for the historical, RCP4.5 and RCP8.5 scenarios as per IPCC (2013). The overall impacts of climate change were evaluated by computing changes in crop water use and yields between historical and future scenarios while assuming no changes in current management practices. The analysis was extended to include assessing the suitability of future climate to both crops by analyzing the proportion of time in which future temperatures will exceed the critical thresholds beyond which crop yields begin decline. These thresholds were obtained from the studies of Adhikari et al. (2015) for sugarcane and Lobell et al. (2011) for maize.

3. Results and discussion

3.1. Model representation of crop evapotranspiration

The performance of the model was first hydrologically evaluated using river flow data and found to exhibit good performance as presented in the Supplementary section, Figure 1.

Similarly, analysis of mean monthly ET averaged over 2009–2014 shows that the model simulations are temporally consistent with WaPOR ET, adequately capturing the crop growing seasons, as shown in Fig. 4. The simulations present overall good predictions and low error statistics with RMSE values of 8.95 mm/yr (maize) and 12.87 mm/yr (sugarcane). Comparatively, sugarcane exhibited a more subtle variation in ET throughout the year, reflecting the perennial growth conditions for the crop. While the model presents a plausible spatial representation of ET, the slight inconsistencies can be explained by the homogenized representation of land cover in SWAT+ as the model was set up to only simulate the growth of one crop for each land cover class. In reality, land cover is with a mix of several cultivated crops and natural vegetation, which yield different amounts of ET. Discrepancies between the simulations and WaPOR can also be explained by uncertainties in the exact timing and execution of crop management practices such as the beginning of planting. The exact timing of other farm management practices,

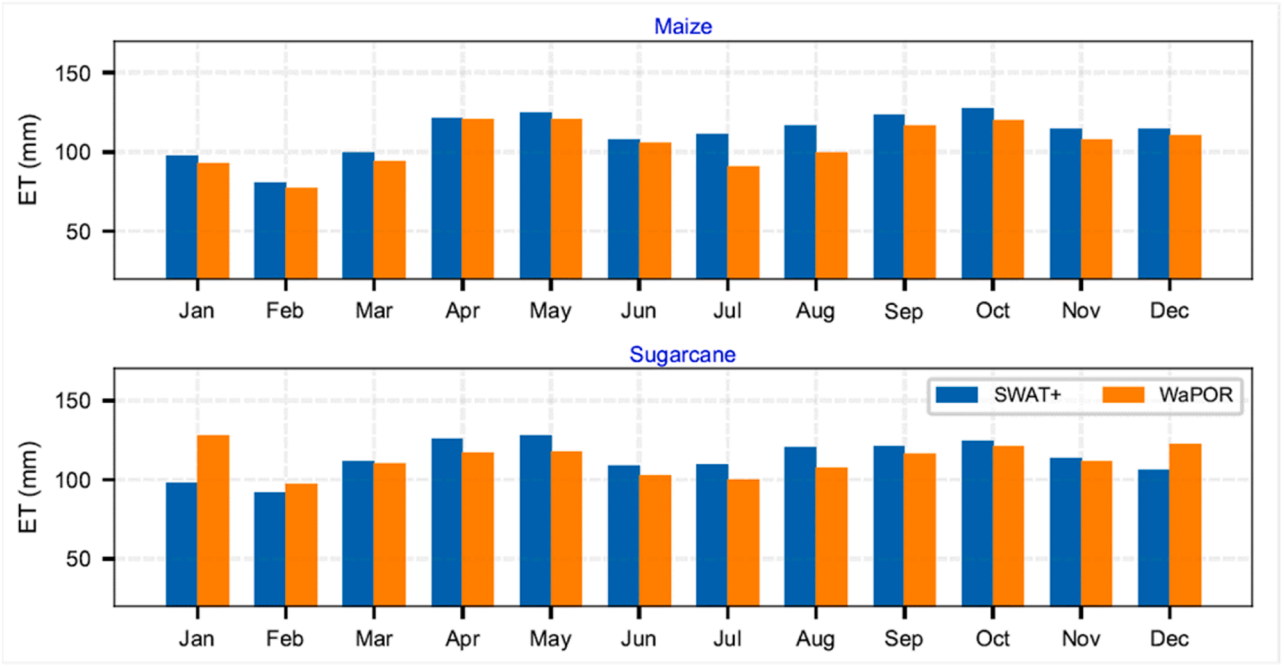

Fig. 4. Comparison of average monthly WaPOR and SWAT+ crop ET. The plots are based on average monthly ET values for the period 2009–2014 where both datasets overlap.

for instance fertilizer application, which have the potential to modify the default crop phenology (e.g., leaf area index and time to maturity) could explain the variations between the two datasets. Additionally, SWAT+ and WaPOR estimate ET using different approaches. On the one hand, SWAT+ employs a water balance approach where ET simulations are dependent on the availability of precipitation. On the other, WaPOR derives ET from an energy balance approach that partitions land surface temperature into latent, sensible, and soil heat fluxes (Blatchford et al., 2020). According to Velpuri and Senay (2017), the difference in the physical parameterization of water balance models and energy balance models can cause inconsistencies in ET estimates especially in irrigated areas, where the uncertainty is further compounded by the estimation of irrigation water application.

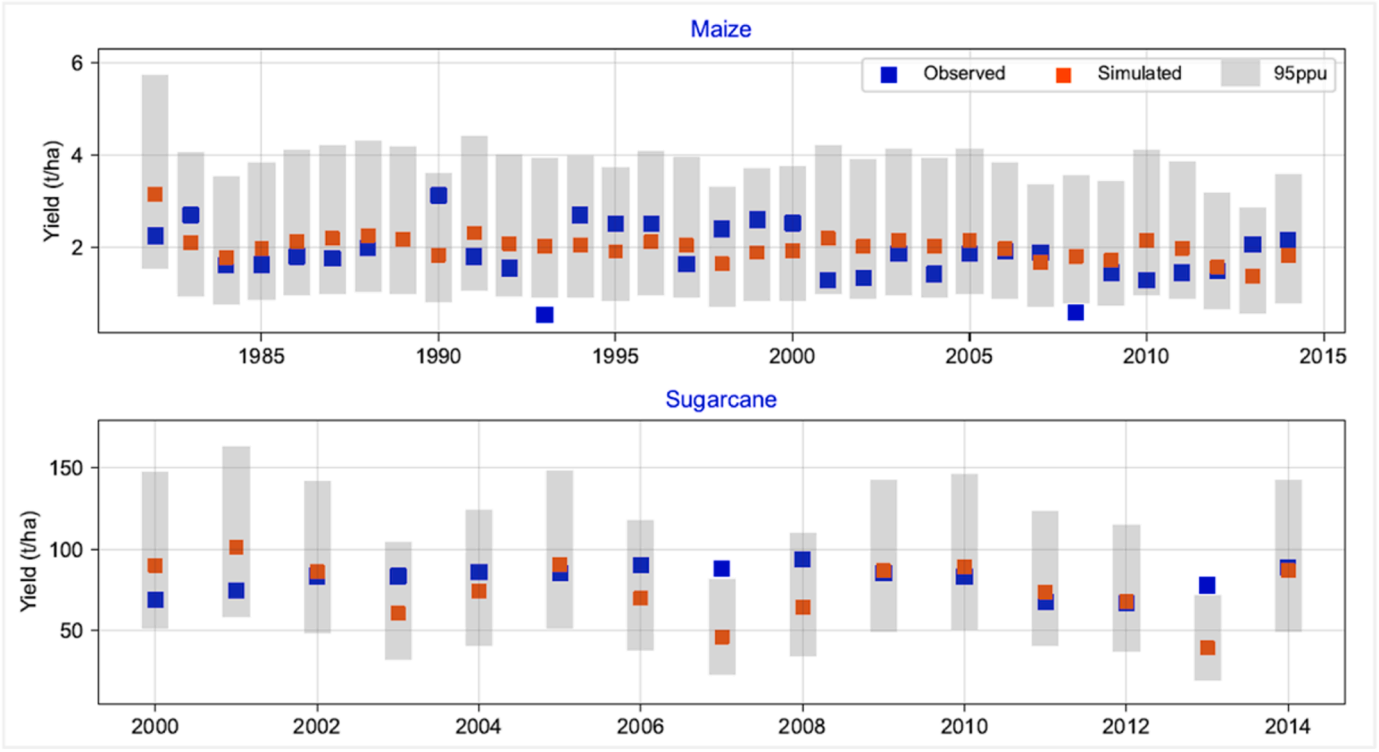

Fig. 5. Plot of annual simulated and observed crop yields. The gray shading represents a 95% prediction uncertainty bound of the simulated yields.

3.2. Crop yield simulation

The calibrated model presented robust predictions of crop yields when evaluated against observations over the overlap periods between the baseline model and the FEWSNET and FAOSTAT datasets. As shown in Fig. 5, the model results exhibit good temporal agreement with the observations as well as good correspondence in the magnitude of yields for the respective crops. Simulated annual average yields were determined to be 2.03 tons ha^{-1} and 81.4tons ha^{-1} for maize and sugarcane respectively. For both crops, the simulated yields fall within the range of observed typical to the region: 0.5–2.5 tons ha^{-1} for maize (Tittonell et al., 2007) and 60–90 tons ha^{-1} for sugarcane (Amolo et al., 2017). The adjusted crop yield parameters are all presented in the Supplementary segment.

Similar to other regions of Kenya, maize yields in the Nyando region show a somewhat stagnated growth and are generally below average global maize yields which have steadily increased from 3.9tons ha^{-1} in 1993–95 to 5.8tons ha^{-1} in 2017–19 (Erenstein et al., 2022. Mumo et al. (2018) report that between 1980 and 2010, maize yields in Kenya have been declining at a rate of about 0.07tons ha^{-1} every decade, with increasing incidences of below average yields since 1995. The study attributes these changes to climate variability-increasing temperatures and decreasing rainfall during the main growing season, the decrease of high potential production areas and financial constraints to acquiring new technology to improve productivity. As with maize, sugarcane yields in Kenya have reduced in recent years, driven by declining soil nutrients and sub-optimal agricultural management practices (e.g. the continued reliance on rainfed production), low-quality sugarcane varieties, the withdrawal of fertilizer subsidies and poor pricing (Waswa et al., 2012; Khaemba et al., 2021).

3.3. Projected changes in temperature and rainfall under climate change

The catchment is projected to undergo an average warming of 2.1°C under RCP4.5 (19.3°C–21.4°C) which more than doubles to 4.6°C under RCP8.5 by which mean temperatures will increase up to 23.9°C at the end of the century (Fig. 6). Multimodel ensemble mean precipitation indicate divergent changes during the long rains over March-May (MAM) and the short rains over October-December (OND). By the end of the 21^{st} century, projections for the MAM season indicate a drying under both scenarios. Under RCP4.5 the amount of the long rains reduces on average from 515 mm historically to 455 mm-a reduction of 60 mm, while RCP8.5 long rains reduce by 35 mm to 480 mm. Across the main growing season of March to August, the amount of rains also reduces on average from 921 mm to 755 mm (− 18%) under RCP4.5 and 813 mm (− 12%) under RCP8.5. On the other hand, both scenarios indicate wetter conditions during the short rainy season, with projected increases of ca. 70 mm under RCP4.5 (a 22.5% increase from 311 mm) and a stronger increase signal of 180 mm (+58%) under RCP8.5. These changes translate to a marginal increase in the total annual precipitation by about 3% under RCP8.5 and a near negligible change (< 1%) under RCP4.5, concurrent with Ogega et al. (2020) who find a decline of about 0.2 mm/day for the MAM rainfall and project an increase of 0.5 mm/day in OND rainfall for the period 2071–2099 relative to 1977–2005. Endris et al. (2019), comparing rainfall changes for the period 2070–2099 relative to 1976–2005, similarly determine drying trends over the western parts of Kenya during the MAM season and an increase in OND precipitation, realizing a larger variability of changes under RCP8.5 than RCP4.5. Similar patterns of change to seasonal precipitation in East Africa have also been reported by Cook and Vizy (2013) who establish that mid-21^{st} century precipitation over the Southern Kenya-Tanzania region reduces by 20–30% during the March-May season compared to corresponding period in the 20^{th} century. The study also finds that 21^{st} century OND precipitation will increase, with precipitation rates increasing on average by 2–4 mm/day. The authors attribute the seasonal change patterns to two factors namely: enhanced moisture advection towards the Congo basin under future climate simulations which leads to a net decrease of the MAM precipitation, and a northeastward shift of the South Indian Convergence Zone- a land-based convergence region characterized by increased rainfall occurring off the southeast coast of southern Africa during the austral summer, which increases the amount of the OND precipitation amount. Consistently, (Shongwe et al., 2011), using a set of 12 coupled general circulation model simulations (CGCMs) from the Coupled Model Intercomparison Project, phase3 (CMIP3) under the A1B emission scenario, project an increase of more than 10% in mean precipitation over majority of the East African region during OND, although Lake Victoria region was not large enough to be adequately resolved by the lowest resolution CGCM. Contrary to the other studies so far referenced, this study finds that MAM precipitation over much of East Africa will increase by about 15%. The authors however report a poor performance of the models in simulating 20^{st} century climate for the same season due to the difficulty in modelling internal atmospheric variations, whose uncertainty during MAM was reported to be higher than in the OND season.

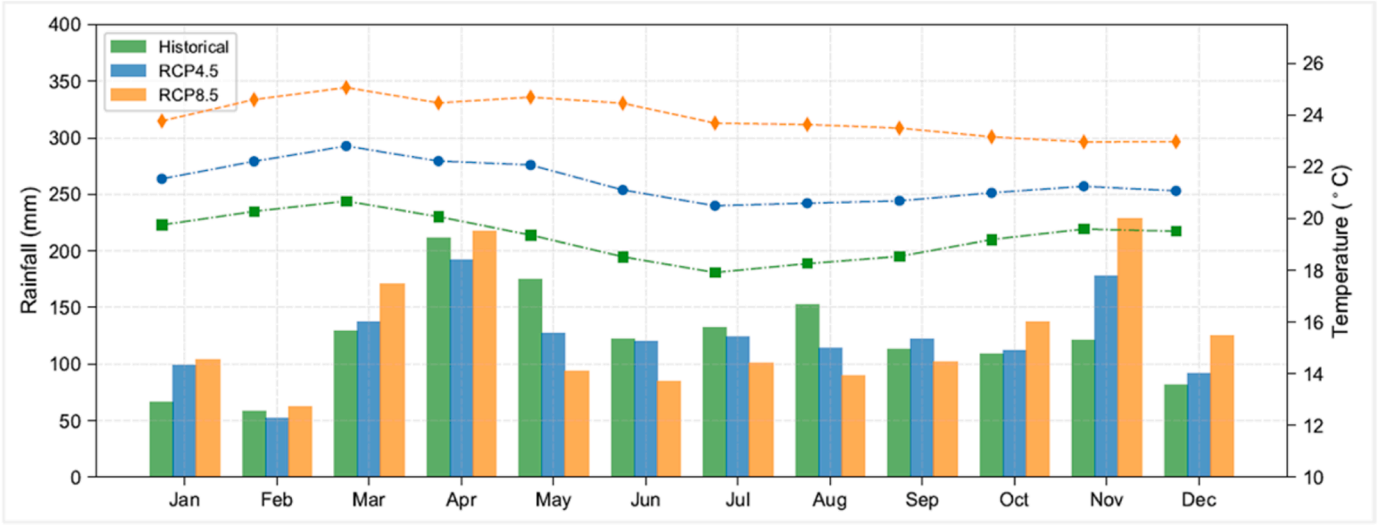

Fig. 6. Projected changes in average monthly temperature (dotted lines) and precipitation (vertical bars) between the historical period 1981–2005 and RCPs 4.5 and 8.5 over 2076–2100.

3.4. Climate change effect on crop water consumption

Temperature-driven increase in atmospheric water demand drives increases the potential evapotranspiration by about 15% and 20% under RCPs 4.5 and 8.5 respectively. Accordingly, the analysis revealed even with the effects of CO_2 accounted for in the future scenarios, the overall signal of actual crop water consumption is still an increase when compared to historical ET. By the end of the century, the water consumption of maize will increase by 106 mm under RCP4.5, which represents a 14% increase from the 1981–2005 amounts. Under the same scenario, sugarcane ET will increase by 64 mm, a 5% increase from the historical period. Climatic conditions under RCP8.5 favor even higher increases in crop water consumption with increases of 21.5% and 8.5% for maize and sugarcane respectively (Fig. 7).

Although seemingly modest, these changes mask the significance of the increase when contrasted with rainfall distribution in the catchment. For context, a projected increase of maize crop ET by 106 mm under RCP4.5 would constitute 25% of all precipitation received during the long rainy season, whose amount is projected to reduce under future climate. The net increase in crop water consumption occurs despite an expected greater economization of water use resulting from reductions in stomatal conductance induced by increased atmospheric CO_2, (− 18% (RCP4.5) and − 51% (RCP8.5) as derived from Equation (6)), indicating that this beneficial response is counteracted by other competing processes and ET-enhancing atmospheric conditions. As temperatures rise, the saturation vapor pressure of the atmosphere increases, thus increasing its capacity to hold more moisture and consequently driving higher evapotranspiration rates. Hatfield et al. (2011) report that while increasing atmospheric CO_2 can reduce water consumption at leaf scale, these effects are downscaled at the plant and ecosystem scale due to a number of competing processes that dampen the positive effects of CO_2 on water use efficiency and soil water retention. Exposure to higher temperatures under future climate increases crop canopy temperature which subsequently increases leaf-to-air vapor pressure gradient, thereby increasing the demand for moisture (Hatfield et al., 2011; Adhikari et al., 2015), to the effect of diminishing the CO_2-induced benefits to crop water use. Through experimental studies Allen et al. (2003), demonstrated that CO_2-induced water use efficiency decreases at higher temperatures. Hatfield and Dold (2019) similarly report that increasing CO_2 at moderate temperatures can increase water use efficiency. However, at temperatures above the optimum species temperature, these positive effects diminish. This would explain why, despite an increase of atmospheric under CO_2 increasing by more 50% under RCP4.5 and more than doubling (124%) under RCP8.5, water use by both maize and sugarcane still increased (Fig. 7).

Changes in relative humidity and vapor pressure associated with reduced precipitation during the long rainy season, combined with positive crop responses to increased CO_2 concentration e.g. increased water use due to bigger leaves, all similarly have an enhancing effect on crop water consumption. Idso et al. (1993) reports that although reduced stomatal conductance has a beneficial effect on water efficiency, it lowers the latent heat flux to the effect of increasing foliage temperature and vapor pressure difference at the plant-atmosphere interface. This acts as a positive feedback on crop water use, which offsets the positive effects of stomatal closure on crop water consumption efficiency. Polley (2002) explains that these feedbacks almost entirely negate the positive effects of a 20–60% reduction in canopy conductance on crop water use.

On the whole, these changes imply that climate change driven increase in crop water consumption, unless accompanied by farm-level water conservation measures or irrigation, are likely to accelerate soil moisture depletion and potentially predispose crops to water and heat stress, particularly as the rainfall received during the main rainy season is projected to decrease. The next section explores in detail the extent to which these climatic changes affect crop yields.

3.5. Effects on crop yields

In both scenarios, maize yields are projected to reduce, with steeper yield reductions under RCP8.5. Under RCP4.5 over the 2076–2100 horizon, climate change is projected to suppress maize yields by 23.9% relative to 1981–2005, from 2.0 ± 0.16 tons ha^{-1} to 1.53 ± 0.10 tons ha^{-1} (Fig. 8). The analysis shows an even stronger reduction of yields under RCP8.5, by which maize yields reduce to 1.54 ± 0.12 tons ha^{-1} (− 29.4%), even though both the precipitation and the amount of atmospheric CO_2 concentration are higher in this scenario compared to RCP4.5. Similar to maize, the simulations under future climate conditions indicated that sugarcane yields are projected to decline (Fig. 8). Under RCP4.5, sugarcane yields are projected to reduce by 18% (from 81.4 ± 12.1 tons ha^{-1} to 67.6 ± 5.2 tons ha^{-1}) and up to 28.6% (to 57.82 ± 7.2 tons ha^{-1}) under a 4.6°C warming projected under RCP8.5.

Correlation plots to disaggregate the relative contributions of rainfall variability and temperature increase on crop yields indicate that in both scenarios rainfall plays a minor role in explaining the declines in crop yields. Fig. 9 shows that for both maize and sugarcane there is little to no correlation between the yields and future rainfall. Moreover, while the mean annual rainfall under RCP8.5 is higher than that under RCP4.5, the correlation between rainfall and yields is nearly identical for both scenarios, emphasizing that rainfall variability does not sufficiently explain the variation between crop yields under the two scenarios. Even though rainfall during the main growing season is projected to reduce under future climate, the magnitudes of change do not appear to be significant enough to harm crop yields. It is also likely that the rainfall increase in the short rainy season will compensate for yield decreases accruing from the reduction in the main rainy season.

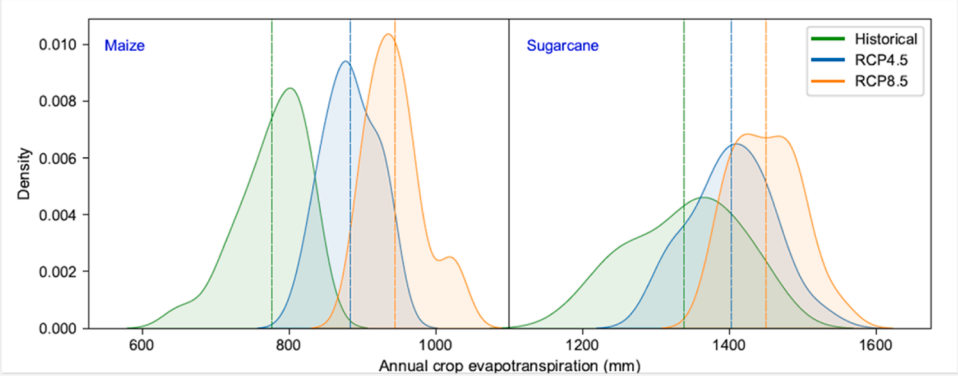

Fig. 7. Plots of annual crop ET for historical, RCP4.5 and RCP8.5 scenarios for maize and sugarcane as kernel density plots. The vertical dashed lines represent the mean ET for each scenario.

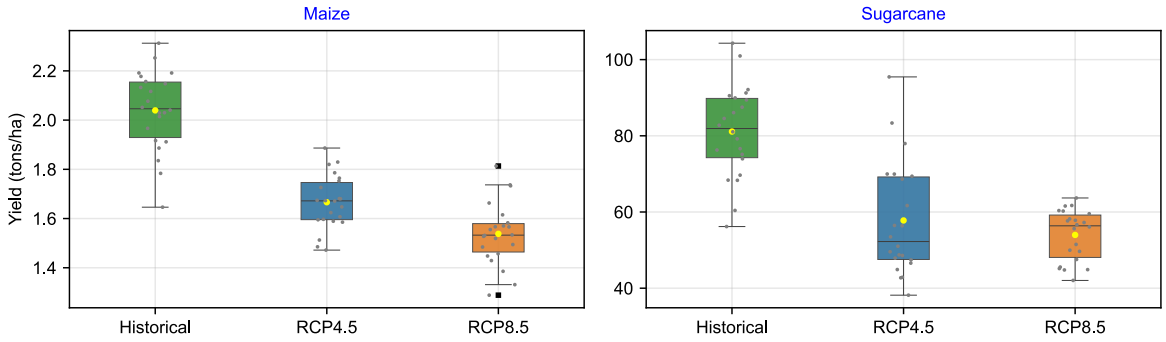

Fig. 8. Projected changes in maize and sugarcane yields between the historical period and end of the 21st century RCP4.5 and RCP8.5 scenarios.

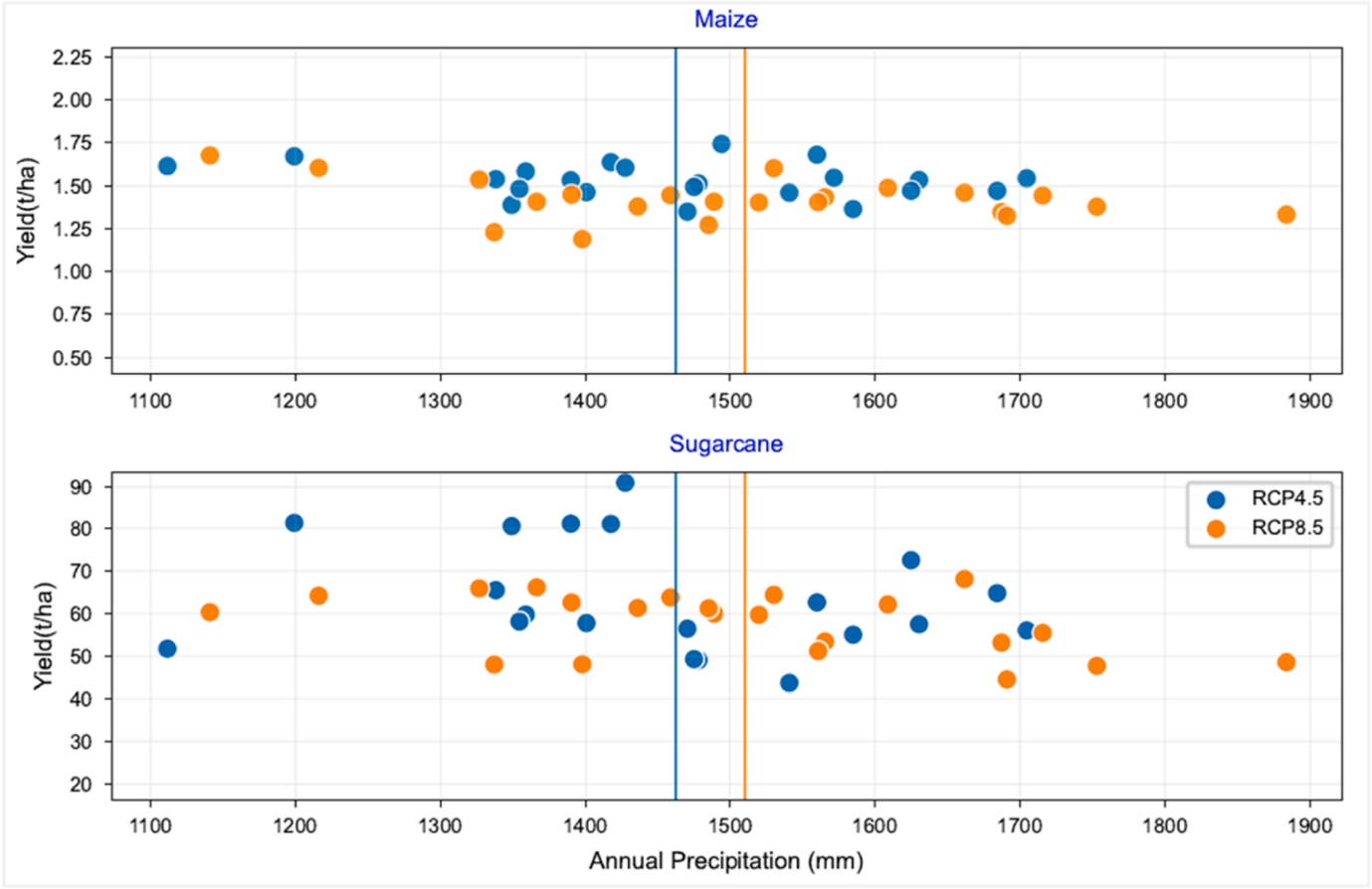

Fig. 9. Scatter plots of annual precipitation and crop yields for RCPs4.5 and 8.5. The vertical lines represent the mean annual rainfall for each scenario and are colored similar to the scenario scatter plots.

When assessing the effect of temperature on crop yields, there is a stronger evidence that the effects of temperature increase have a deleterious effect on crop yields. From Fig. 10, it is apparent that temperature increase, to a larger extent than precipitation, explains the future reduction of both maize and sugarcane yields. The yields are plotted against scenario temperature anomalies for RCP4.5 and RCP8.5 and the corresponding coefficients of determination indicate that temperature has a stronger effect in explaining the yield reductions. Temperature increase explains 67% ($p = 0.0000028$) of the variance in maize yields under RCP4.5 and 44% ($p = 0.0072$) of the variance under RCP8.5. It is probable that the lower variance explained by temperature under RCP8.5 is due to the effect of higher atmospheric CO_2, which slightly dampens the effects of temperature. Nevertheless, the signal of increasing temperature on the crop yields is still clearly visible. The gradient of decline of yields under increasing temperature for both scenarios is nearly equal (−0.14ton/ha/°C (RCP4.5) and − 0.13ton/ha/°C (RCP8.5)). These findings are consistent with Lobell and Burke (2008), who find that due to the magnitude of future warming, the negative effects of future temperature rise on crop yields will outweigh the effects of rainfall variability.

For sugarcane, temperature has a near negligible contribution to the variance in yields compared to maize under RCP4.5, with a much lower correlation coefficient of 0.05 ($p = 0.31$). This could arise from the fact that sugarcane exhibits a higher optimum temperature compared to maize and is comparatively less affected by smaller temperature increases (Adhikari et al., 2015). However, under RCP8.5, when temperature increases exceed the optimum range, the proportion of the variance of sugarcane yields explained by temperature increases

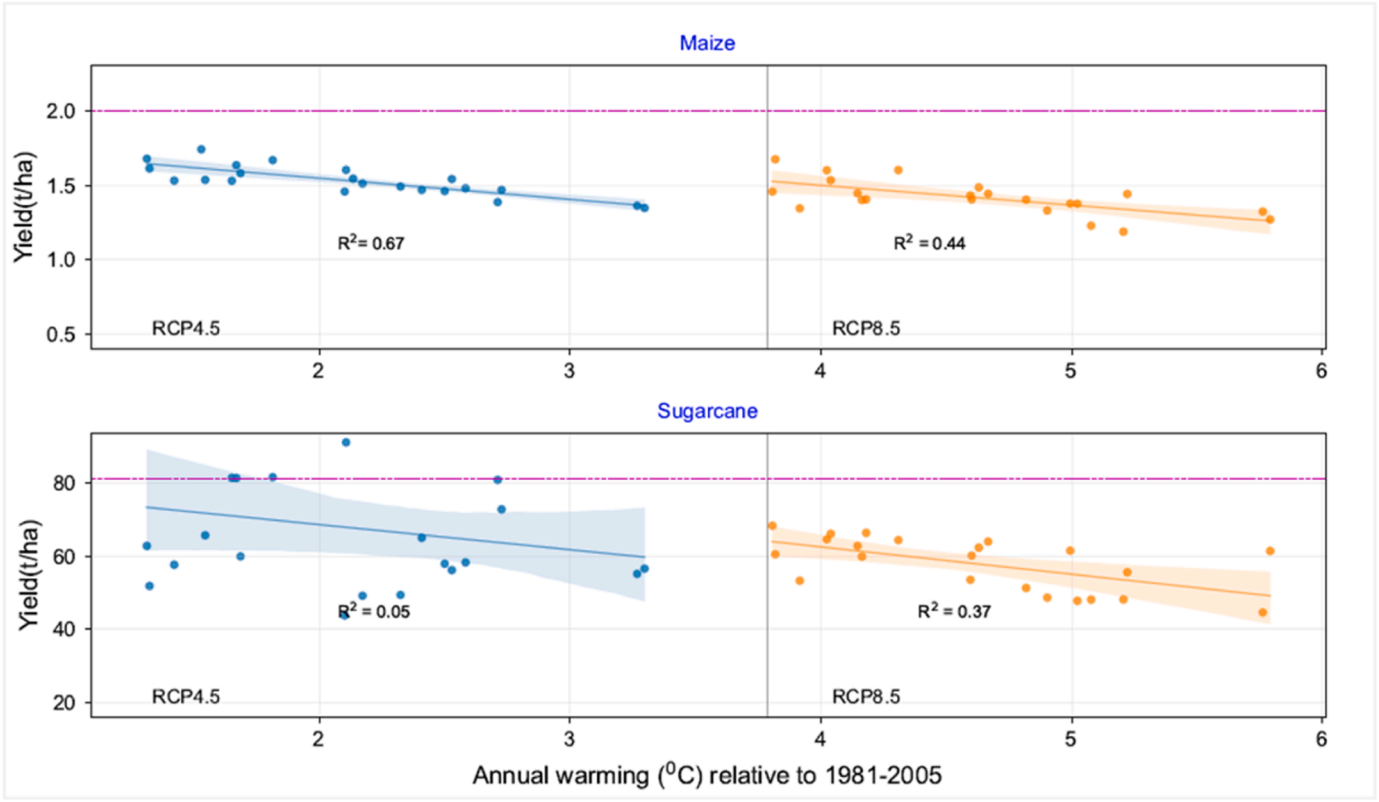

Fig. 10. Correlation plots of annual temperature anomaly and crop yields for RCPs 4.5 and 8.5. The horizontal dashed magenta lines represent the average crop yields for the historical period.

substantially(R^2 = 0.37, p = 0.0029). A higher thermal tolerance of sugarcane would also explain why the proportion of drop in yields is less than that observed for maize.These negative trends in the yields of maize and sugarcane are consistent with the fact both are C_4 crop species and their photosynthetic activity is not expected to significantly benefit from CO_2 fertilization (Leakey et al., 2006).

The amount of area harvested for each crop does not show any trend of decrease since the threshold for the controlling factors of planting such as the amount of moisture to trigger planting are still met. Since the harvesting of sugarcane is controlled by the time to crop maturity, the amount of area harvested varies according to the amount of plant biomass removed from harvesting mature crops in the previous harvest. For maize, the area is constant since harvesting is defined by calendar days and all harvest operations are carried out simultaneously. The plots of harvest areas are provided in the Supplementary section.

On the suitability of future climate to both crops, there is a projected increase in the frequency of temperatures that have adverse effects on physiological plant processes. Lobell et al. (2011) report that for every growing degree day exceeding 30˚C, yields of tropical maize in Africa decrease by around 1% under optimal rainfed conditions, with a higher reduction of 1.7% occurring during drought conditions. The continued exposure of maize to such high temperatures explain the reduction in yields which result from a number of physiological changes. Hatfield (2016) reports that continual exposure to temperatures above 30˚C during the pollination stage reduces the kernel numbers while exposure to high night time temperatures during the grain filling stage shortens the grain-fill period due to increased senescence. Concurrently, Hatfield et al. (2011) report that exposure to higher temperatures accelerates the development of annual crops. This leads to smaller plant sizes and a shortened reproductive phase that ultimately translates to reduced grain yields. At temperatures above 35˚C, the viability of maize pollen decreases, ovary fertilization is suppressed and the subsequent growth rate of kernels reduces even if temperatures dropped at later growth stages. Comparable findings of Ben-Asher et al. (2008), which studied the effects of extreme temperature on the development of sweet corn, report that photosynthetic rates of sweet corn are highest at the 20–25˚C temperature range but would reduce by 50–60% were the temperatures to increase to the 35–40˚C range. During the reproductive stage, heat stress can cause the parchedness of silks, increase pollen sterility and poor seed setting (Sánchez et al., 2014).

Analysis of the projected temperatures under the future climate scenarios reveals that the average number of days where maximum daytime temperatures exceed 30˚C in the Nyando region is projected to increase significantly from 10.5% in the historical climate to 32% under the RCP4.5 scenario. Under the more extreme RCP8.5 scenario, this frequency will increase six-fold to 66%, underlining the extent of adversity that crops are anticipated to face (Fig. 11). Based solely on these statistics, this would mean that under the high emission scenario, maize growth in the Nyando region will only be above sub-optimal conditions for approximately one-third of the time. This is corroborated by Ojara et al. (2021) who find that the climate suitability of maize growing areas in western Kenya will reduce by 20–40% under future climate.

Within the larger Lake Victoria region, maize yield declines under future climate have also been observed by Bwambale and Mourad (2022) and Nkwasa et al. (2023). The latter determining that over the period 2071–2100 relative to 1971–2000, maize yields over the entire Lake Victoria region will reduce by 17.5 ± 1.9% if cultivar adaptations are not implemented. Davenport et al. (2018) report maize yield reductions of 7% in Western Kenya although their analysis is based on projected trends until 2026–2040. On a broader regional perspective, Adhikari et al. (2015) report that under different temperature-maize yield relationships, maize yields in Eastern Africa are projected to reduce by anywhere between 6% and 40% under the A2 emission scenario.

For sugarcane, climatic conditions under both scenarios are also

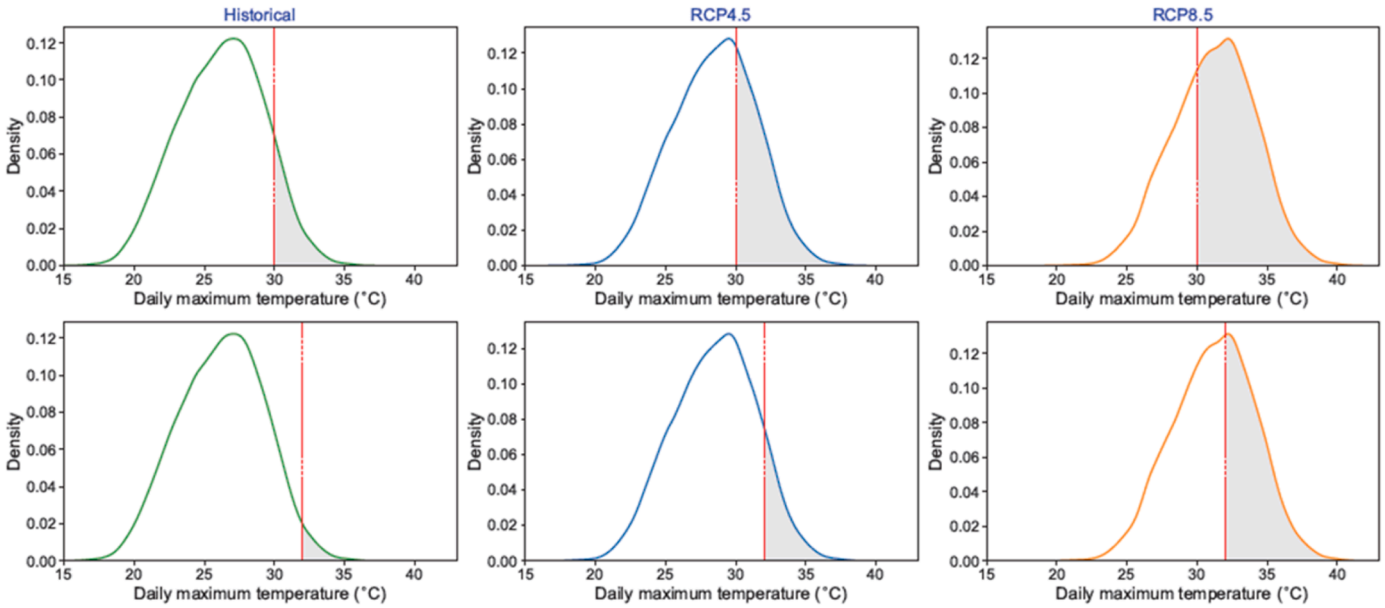

Fig. 11. Kernel density estimation plots of daily maximum temperatures for the three scenarios. For each scenario, the gray shaded area represents the proportion of time where maximum daily temperatures exceed thresholds beyond which temperatures become detrimental to crop yields, and correspond to 30°C (Lobell et al., 2011) for maize (top row) and 32°C (Adhikari et al., 2015) for sugarcane, displayed on the bottom row.

projected to inhibit growth. Sugarcane is reported to thrive at temperatures between 30 and 32°C, beyond which sucrose yields decline, while temperatures beyond 35°C are harmful to growth (Chandiposha, 2013; Adhikari et al., 2015. Wahid (2007), found that when exposed to heat stress (ca. 40°C), sugarcane dry matter and leaf area was greatly reduced. Heat stress also hindered the capability of sugarcane to absorb and assimilate nutrients and CO_2 to produce dry matter. Flack-Prain et al. (2021) similarly found that increased temperature enhances sugarcane development but reduced the assimilation of Carbon. Although high temperatures increase early-stage leaf area of sugarcane, higher leaf turnover reduced late season leaf area and consequently the gross primary productivity. Sonkar et al. (2019) report that when exposed to a temperature rise of 1–4°C, fresh sugarcane stalk biomass and sucrose mass decreased by 2–25%. On this account, conditions within the Nyando catchment are projected to increasingly limit sugarcane productivity, as mean daily maximum temperatures exceeding 32°C will be surpassed on average 12% of the time under RCP4.5% and 42% under RCP8.5 (Fig. 11). Another consideration in the performance of sugarcane in the future is the occurrence of droughts. As with other crops, the projected increase in the frequency of droughts in the East Africa region under climate change is expected to limit water availability and negatively affect sugarcane.

There is limited literature on the effects of climate change on sugarcane yields in East Africa. Waithaka et al. (2013) argue that since it is a C_4 crop, sugarcane should exhibit the same productivity responses as maize when grown in the same geographic regions. Lobell et al. (2008) determine that by 2030, sugarcane yields in the East African region will undergo a decline of less than 10% relative to the 1998–2002 average yields. According to Adhikari et al. (2015), the productivity of rainfed sugarcane in the region will largely depend of water availability and the magnitude of future warming.

3.6. Limitations of the study

The findings of this study, despite showing consensus with related studies, are constrained by some limitations. First, the availability of the full range of climate outputs to run the SWAT+ model limited the selection to only five RCMs and although the results are reported as a multi-model ensemble average, this subset of models might not cover the full range of RCM uncertainty under future climate. Uncertainties also exist with regards to the quality of outputs of the RCMs themselves. Adachi et al. (2019) report that despite RCMs reducing the climate bias from general circulation models (GCMs), RCMs still inherit the climate change signal from the GCMs and can even show a different downscaled climate under the same boundary conditions and model configurations. There are also uncertainties in the magnitude and direction of projected precipitation changes over East Africa by CORDEX-AFR RCMs as reported in Bichet et al. (2020). The study observed a significant dispersion in the direction of projected precipitation among RCMs, resulting in an overall low confidence in the trends. Similar to climate models, the choice of crop models is also an important source of uncertainty in assessing the agricultural impacts of climate change and can explain the variance in projected changes in crop productivity, with almost a similar contribution to the total uncertainty as the climate models (Müller et al., 2021). The cumulative effect of CO_2 fertilization is another source of uncertainty in the results. Although the model shows greater sensitivity to CO_2 fertilization under RCP8.5, these changes are reported with caution, as the effects of an atmospheric CO_2 concentration of 827 ppmv under this scenario falls outside the range of 330–660 ppmv, within which the equations used in SWAT+ to derive radiation-use efficiency and stomatal conductance are valid. As reported by Müller et al. (2021), the effects of CO_2 fertilization have been found to be an important source of disagreement between different crop models when assessing the effects of climate change on different crops and the representation of the full effects of CO_2 fertilization in models remain a subject of great debate.

In addition, the simulation in this study adopts a climate-only, limited-adaptation approach, assuming that current management practices will remain in place under future climate. Although planting is scheduled according to moisture availability and will thus shift with the rains, there is a broader assumption that farmers will persist with rainfed crops, continue with the current crop varieties or maintain cultivation in areas where climate is too adverse for crops. However, the expectation is that under permitting conditions, farmers will respond by utilizing irrigation, adopt more resistant and higher yielding varieties or modify cropping systems. Nkwasa et al. (2023) demonstrate for instance that by adopting late maturing varieties, farmers within Lake Victoria region can mitigate climate change-induced maize yield losses.

Climate change is also expected to impact crop yields in ways that are not fully accounted for in this study. As noted previously, the frequency of high temperatures is anticipated to increase within the study area. The extent to which the consequent heat stress will impact crop yields remains partially uncertain, nonetheless, heat stress will be an important factor on crop yields under future climate (IPCC, 2022). Teixeira et al. (2013) outline that heat stress can cause severe damage in crops, particularly if its occurrence coincides with the reproductive stage. Finally, climate change is expected to increase the proliferation of weeds, pests and diseases (IPCC, 2022), which will negatively affect yields yet the magnitudes are difficult to quantify.

4. Conclusions

This study has applied downscaled climate data to assess the agricultural impacts of climate change in a data scarce catchment. The results suggest that climate change will pose increasingly detrimental conditions to the performance of maize and sugarcane in the Nyando region. In both RCPs 4.5 and 8.5, there will be a marked increase in the frequency of temperatures exceeding the optimal thresholds of both crops indicating more adverse conditions under which crops are anticipated to face. Aggregating the combined effects of precipitation change, temperature increase and no adaptation to future conditions, annual maize yields are projected to decline by 23.9% and 29.4% under RCP4.5 and RCP8.5 respectively, while sugarcane yields will reduce by 17% and 28.6% under both scenarios respectively. The analysis indicates that future warming outweighs the effects of precipitation variability in explaining the decline in crop yields. These results indicate the nature of challenges climate change is anticipated to impose on agriculture in a region already characterized by low productivity, adaptive capacity and disproportional exposure to the effects of climate. While there is general consensus that crop performance will deteriorate under future climate in the region, the full extent of variance can be determined by utilizing a wider range of climate and crop simulation models and quantifying the impacts of climate change from a wider scope beyond only climatological conditions. Although applied to one catchment, the methodology and datasets are sufficiently robust to be readily applied to any data scarce catchment in the region.

Author contributions

AN, AvG and KL formulated the study. KL, AN and LV set up the model and performed the simulations. KL analyzed the data and prepared the manuscript with contributing reviews and revisions from all authors. All authors read and approved the contents of the final manuscript.

Funding

The authors acknowledge the financial support of the Research Foundation - Flanders (FWO) for funding the International Coordination Action (ICA) “Open Water Network: Open Data and Software tools for water resources management” (project code G0E2621N).

CRediT authorship contribution statement

Lekarkar Katoria Lesaalon: Writing – review & editing, Writing – original draft, Software, Methodology, Investigation, Formal analysis, Data curation, Conceptualization. **Nkwasa Albert:** Writing – review & editing, Conceptualization. **Villani Lorenzo:** Writing – review & editing, Software, Formal analysis. **van Griensven Ann:** Writing – review & editing, Resources, Funding acquisition, Conceptualization.

Declaration of Competing Interest

The authors declare that they have no known competing financial interests or personal relationships that could have appeared to influence the work reported in this paper.

Data Availability

Data will be made available on request.

Appendix A. Supporting information

Supplementary data associated with this article can be found in the online version at doi:10.1016/j.agwat.2024.108696.

References

Abbaspour, K.C., Rouholahnejad, E., Vaghefi, S., Srinivasan, R., Yang, H., Kløve, B., 2015. A continental-scale hydrology and water quality model for Europe: calibration and uncertainty of a high-resolution large-scale SWAT model. J. Hydrol. 524, 733–752. https://doi.org/10.1016/j.jhydrol.2015.03.027.

IPCC, 2022. Climate change 2022: impacts, adaptation and vulnerability. In: Pörtner, H.-O., Roberts, D.C., Tignor, M., Poloczanska, E.S., Mintenbeck, K., Alegría, A., Craig, M., Langsdorf, S., Löschke, S., Möller, V., Okem, A., Rama, B. (Eds.), Contribution of Working Group II to the Sixth Assessment Report of the Intergovernmental Panel on Climate Change. Tech. rep., Cambridge, UK and New York, NY, USA. https://doi.org/10.1017/9781009325844.

IPCC, 2013. In: Stocker, T.F., Qin, D., Plattner, G.-K., Tignor, M., Allen, S.K., Boschung, J., Nauels, A., Xia, Y., Bex, V., Midgley, P.M. (Eds.), Annex II: Climate System Scenario Tables:[Prather, M., G. Flato, P. Friedlingstein, C. Jones, J.-F. Lamarque,H. Liao and P. Rasch (eds.)]. In: Climate Change 2013: The Physical Science Basis. Contribution of Working Group I to the Fifth Assessment Report of the Intergovernmental Panel on Climate Change. Cambridge University Press, Cambridge, United Kingdom and New York, NY, USA.

Abrams, L. Unlocking the potential of enhanced rainfed agriculture, Tech. rep., Stockholm International Water Institute, Stockholm, 2018.

Adachi, S.A., Nishizawa, S., Ando, K., Yamaura, T., Yoshida, R., Yashiro, H., Kajikawa, Y., Tomita, H., 2019. An evaluation method for uncertainties in regional climate projections. Atmos. Sci. Lett. 20, e877.

Adhikari, U., Nejadhashemi, A.P., Woznicki, S.A., 2015. Climate change and eastern Africa: a review of impact on major crops. Food Energy Secur. 4, 110–132.

Alemayehu, T., Van Griensven, A., Woldegiorgis, B.T., Bauwens, W., 2017. An improved SWAT vegetation growth module and its evaluation for four tropical ecosystems. Hydrol. Earth Syst. Sci. 21, 4449–4467. https://doi.org/10.5194/hess-21-4449-2017.

Allen, L., Pan, D., Boote, K., Pickering, N., Jones, J., 2003. Carbon dioxide and temperature effects on evapotranspiration and water use efficiency of soybean. Agron. J. 95, 1071–1081.

Allen, R.G., Pereira, L.S., Raes, D., Smith, M., et al., Crop evapotranspiration-Guidelines for computing crop water requirements-FAO Irrigation and drainage paper 56, Fao, Rome, 300, D05109, 1998.

Amolo, R.A., Sigunga, D.O., Owuor, P.O., 2017. Evaluation of soil properties of sugarcane zones and cropping systems for improved productivity in Western Kenya. Int. J. Agron. Agric. Res.

Baron, C., Sultan, B., Balme, M., Sarr, B., Traore, S., Lebel, T., Janicot, S., Dingkuhn, M., 2005. From GCM grid cell to agricultural plot: scale issues affecting modelling of climate impact. Philos. Trans. R. Soc. B: Biol. Sci. 360, 2095–2108.

Beck, H.E., Zimmermann, N.E., McVicar, T.R., Vergopolan, N., Berg, A., Wood, E.F., 2018. Present and future Köppen-Geiger climate classification maps at 1-km resolution. Sci. data 5, 1–12.

Beck, H.E., Van Dijk, A.I., Larraondo, P.R., McVicar, T.R., Pan, M., Dutra, E., Miralles, D. G., 2022. MSWX: Global 3-hourly 0.1 bias-corrected meteorological data including near-real-time updates and forecast ensembles. Bull. Am. Meteorol. Soc. 103, E710–E732.

Ben-Asher, J., Garcia y Garcia, A., Hoogenboom, G., 2008. Effect of high temperature on photosynthesis and transpiration of sweet corn (Zea mays L. var. rugosa). Photosynthetica 46, 595–603.

Bichet, A., Diedhiou, A., Hingray, B., Evin, G., Touré, N.E., Browne, K.N.A., Kouadio, K., 2020. Assessing uncertainties in the regional projections of precipitation in CORDEX-AFRICA. Clim. Change 162, 583–601.

Bieger, K., Arnold, J.G., Rathjens, H., White, M.J., Bosch, D.D., Allen, P.M., Volk, M., Srinivasan, R., 2017. Introduction to SWAT+, a completely restructured version of the soil and water assessment tool. J. Am. Water Resour. Assoc. 53, 115–130. https://doi.org/10.1111/1752-1688.12482.

Blatchford, M.L., Mannaerts, C.M., Njuki, S.M., Nouri, H., Zeng, Y., Pelgrum, H., Wonink, S., Karimi, P., 2020. Evaluation of WaPOR V2 evapotranspiration products across Africa. Hydrol. Process. 34, 3200–3221. https://doi.org/10.1002/hyp.13791.

Burke, M.B., Lobell, D.B., Guarino, L., 2009. Shifts in African crop climates by 2050, and the implications for crop improvement and genetic resources conservation. Glob. Environ. Change 19, 317–325.

Bwambale, J., Mourad, K.A., 2022. Modelling the impact of climate change on maize yield in Victoria Nile Sub-basin, Uganda. Arab. J. Geosci. 15, 40.

Chandiposha, M., Potential impact of climate change in sugarcane and mitigation strategies in Zimbabwe, 2013.

Chaturvedi, V., Hejazi, M., Edmonds, J., Clarke, L., Kyle, P., Davies, E., Wise, M., 2015. Climate mitigation policy implications for global irrigation water demand. Mitig. Adapt. Strateg. Glob. Change 20, 389–407. https://doi.org/10.1007/s11027-013-9497-4.

Chawanda, C.J., SWAT+ Toolbox User Manual, 10.5281/zenodo.6331716, 2021.

Chen, Y., Marek, G.W., Marek, T.H., Moorhead, J.E., Heflin, K.R., Brauer, D.K., Gowda, P. H., Srinivasan, R., 2019. Simulating the impacts of climate change on hydrology and crop production in the Northern High Plains of Texas using an improved SWAT model. Agric. Water Manag. 221, 13–24.

Cook, K.H., Vizy, E.K., 2013. Projected changes in East African rainy seasons. J. Clim. 26, 5931–5948.

Davenport, F., Funk, C., Galu, G., 2018. How will East African maize yields respond to climate change and can agricultural development mitigate this response? Clim. Change 147, 491–506.

Dinku, T., Funk, C., Peterson, P., Maidment, R., Tadesse, T., Gadain, H., Ceccato, P., 2018. Validation of the CHIRPS satellite rainfall estimates over eastern Africa. Q. J. R. Meteorol. Soc. 144, 292–312.

Duan, Z., Tuo, Y., Liu, J., Gao, H., Song, X., Zhang, Z., Yang, L., Mekonnen, D.F., 2019. Hydrological evaluation of open-access precipitation and air temperature datasets using SWAT in a poorly gauged basin in Ethiopia. J. Hydrol. 569, 612–626.

Endris, H.S., Lennard, C., Hewitson, B., Dosio, A., Nikulin, G., Artan, G.A., 2019. Future changes in rainfall associated with ENSO, IOD and changes in the mean state over Eastern Africa. Clim. Dyn. 52, 2029–2053. https://doi.org/10.1007/s00382-018-4239-7.

Erenstein, O., Jaleta, M., Sonder, K., Mottaleb, K., Prasanna, B., 2022. Global maize production, consumption and trade: Trends and R&D implications. Food Secur. 14, 1295–1319.

FAO, Digital soil map of the world and derived soil properties, Tech. Rep. January, ⟨https://www.FAO.org/soils-portal/data-hub/soil-maps-and-databases/FAOunesco-soil-map-of-the-world/en/⟩, 2003.

FAO, WaPOR V2 quality assessment - Technical Report on the Data Quality of the WaPOR FAO Database version 2, Tech. rep., Rome, 10.4060/cb2208en, 2020.

Farr, T.G., Rosen, P.A., Caro, E., Crippen, R., Duren, R., Hensley, S., Paller, M., Kobrick, M., Rodriguez, E., Roth, L., Seal, D., Shaffer, S., Shimada, J., Umland, J., Werner, M., Oskin, M., Burbank, D., Alsdorf, D., 2007. The shuttle radar topography mission, 10.1029/2005RG000183 Lect. Notes Comput. Sci. (Incl. Subser. Lect. Notes Artif. Intell. Lect. Notes Bioinforma.) 2181, 1–33, 10.1029/2005RG000183.

Flack-Prain, S., Shi, L., Zhu, P., da Rocha, H.R., Cabral, O., Hu, S., Williams, M., 2021. The impact of climate change and climate extremes on sugarcane production. GCB Bioenergy 13, 408–424.

Funk, C., Peterson, P., Landsfeld, M., Pedreros, D., Verdin, J., Shukla, S., Husak, G., Rowland, J., Harrison, L., Hoell, A., Michaelsen, J., 2015. The climate hazards infrared precipitation with stations - a new environmental record for monitoring extremes. Sci. Data 2, 1–21. https://doi.org/10.1038/sdata.2015.66.

Gathenya, M., Mwangi, H., Coe, R., Sang, J., 2011. Climate-and land use-induced risks to watershed services in the Nyando river basin, Kenya. Exp. Agric. 47, 339–356. https://doi.org/10.1017/S001447971100007X.

Gebrechorkos, S.H., Hülsmann, S., Bernhofer, C., 2019. Long-term trends in rainfall and temperature using high-resolution climate datasets in East Africa. Sci. Rep. 9, 11376 https://doi.org/10.1038/s41598-019-47933-8.

Graham, L.P., Andréasson, J., Carlsson, B., 2007. Assessing climate change impacts on hydrology from an ensemble of regional climate models, model scales and linking methods–a case study on the Lule River basin. Clim. Change 81, 293–307.

Hatfield, J.L., 2016. Increased temperatures have dramatic effects on growth and grain yield of three maize hybrids. Agric. Environ. Lett. 1, 150006.

Hatfield, J.L., Dold, C., 2019. Water-use efficiency: advances and challenges in a changing climate. Front. Plant Sci. 10 https://doi.org/10.3389/fpls.2019.00103.

Hatfield, J.L., Boote, K.J., Kimball, B.A., Ziska, L., Izaurralde, R.C., Ort, D., Thomson, A. M., Wolfe, D., 2011. Climate impacts on agriculture: implications for crop production. Agron. J. 103, 351–370.

Idso, S.B., Kimball, B.A., Akin, D., Kridler, J., 1993. A general relationship between CO_2-induced reductions in stomatal conductance and concomitant increases in foliage temperature. Environ. Exp. Bot. 33, 443–446.

Jeyrani, F., Morid, S., Srinivasan, R., 2021. Assessing basin blue-green available water components under different management and climate scenarios using SWAT. Agric. Water Manag. 256, 107074 https://doi.org/10.1016/j.agwat.2021.107074.

Jia, K., Zhang, W., Xie, B., Xue, X., Zhang, F., Han, D., 2022. Does climate change increase crop water requirements of winter wheat and summer maize in the lower reaches of the Yellow River Basin? Int. J. Environ. Res. Public Health 19. https://doi.org/10.3390/ijerph192416640.

Khaemba, P.F., Muiruri, P.W., Kibutu, T.N., 2021. Trend analysis in sugarcane growth in Mumias Sugar Belt, Western Kenya; foR THE Period 1985–2015. Interdiscip. J. Rural Community Stud. 3, 31–40.

Kipkulei, H.K., Bellingrath-Kimura, S.D., Lana, M., Ghazaryan, G., Baatz, R., Boitt, M., Chisanga, C.B., Rotich, B., Sieber, S., 2022. Assessment of maize yield response to agricultural management strategies using the DSSAT-CERES-Maize Model in Trans Nzoia County in Kenya. Int. J. Plant Prod. 16, 557–577. https://doi.org/10.1007/s42106-022-00220-5.

ESA, LandCover CCI Product User Guide Version 2, Tech. rep., ⟨maps.elie.ucl.ac.be/CCI/viewer/download/ESACCI-LC-Ph2-PUGv2_2.0.pdf⟩, 2017.

Le, A.M., Pricope, N.G., 2017. Increasing the accuracy of runoff and streamflow simulation in the Nzoia Basin, Western Kenya, through the incorporation of satellite-derived CHIRPS data. Water 9, 114.

Leakey, A.D., Uribelarrea, M., Ainsworth, E.A., Naidu, S.L., Rogers, A., Ort, D.R., Long, S. P., 2006. Photosynthesis, productivity, and yield of maize are not affected by open-air elevation of CO_2 concentration in the absence of drought. Plant Physiol. 140, 779–790.

Liu, J., Yang, H., 2006. Spatially explicit assessment of global consumptive water uses in cropland: green and blue water. J. Hydrol. 384, 187–197. https://doi.org/10.1016/j.jhydrol.2009.11.024.

Lobell, D.B., Burke, M.B., 2008. Why are agricultural impacts of climate change so uncertain? the importance of temperature relative to precipitation. Environ. Res. Lett. 3, 034007.

Lobell, D.B., Burke, M.B., Tebaldi, C., Mastrandrea, M.D., Falcon, W.P., Naylor, R.L., 2008. Prioritizing climate change adaptation needs for food security in 2030. Science 319, 607–610.

Lobell, D.B., Bänziger, M., Magorokosho, C., Vivek, B., 2011. Nonlinear heat effects on African maize as evidenced by historical yield trials. Nat. Clim. Change 1, 42–45.

Maidment, R.I., Grimes, D., Black, E., Tarnavsky, E., Young, M., Greatrex, H., Allan, R.P., Stein, T., Nkonde, E., Senkunda, S., Alcántara, E.M.U., 2017. A new, long-term daily satellite-based rainfall dataset for operational monitoring in Africa. Sci. Data 4. https://doi.org/10.1038/sdata.2017.63.

Mearns, L., Easterling, W., Hays, C., Marx, D., 2001. Comparison of agricultural impacts of climate change calculated from high and low resolution climate change scenarios: Part I. The uncertainty due to spatial scale. Clim. Change 51, 131–172.

Mengistu, A.G., Woldesenbet, T.A., Dile, Y.T., 2022. Evaluation of observed and satellite-based climate products for hydrological simulation in data-scarce Baro-Akob River Basin, Ethiopia. Ecohydrol. Hydrobiol. 22, 234–245.

Mitchell, T., Tanner, T., Roach, R., and Boyd, S., Adapting to climate change Challenges and opportunities for the development community, ⟨www.ids.ac.uk/ids⟩, 2006.

Msigwa, A., Komakech, H.C., Verbeiren, B., Salvadore, E., Hessels, T., Weerasinghe, I., van Griensven, A., 2019. Accounting for seasonal land use dynamics to improve estimation of agricultural irrigation water withdrawals. Water (Switz.) 11. https://doi.org/10.3390/w11122471.

Mugalavai, E., Kipkorir, E.C., Mugalavai, E.M., Kipkorir, E.C., 2013. Assessing the potential of maize growing seasons for Western Kenya using agroclimatic indices. J. Disaster Manag. Risk Reduct. ⟨https://www.researchgate.net/publication/239084054⟩.

Mulianga, B., Bégué, A., Clouvel, P., Todoroff, P., 2015. Mapping cropping practices of a sugarcane-based cropping system in Kenya using remote sensing. Remote Sens. 7, 14428–14444. https://doi.org/10.3390/rs71114428.

Müller, C., Franke, J., Jägermeyr, J., Ruane, A.C., Elliott, J., Moyer, E., Heinke, J., Falloon, P.D., Folberth, C., Francois, L., Izaurralde, R.C., Jacquemin, I., Liu, W., Olin, S., Pugh, T.A.M., Williams, K., Zabel, F., 2021. Exploring uncertainties in global crop yield projections in a large ensemble of crop models and CMIP5 and CMIP6 climate scenarios. Environ. Res. Lett. 16, 034040.

Mumo, L., Yu, J., Fang, K., 2018. Assessing impacts of seasonal climate variability on maize yield in Kenya. Int. J. Plant Prod. 12, 297–307.

Musie, M., Sen, S., Srivastava, P., 2019. Comparison and evaluation of gridded precipitation datasets for streamflow simulation in data scarce watersheds of Ethiopia. J. Hydrol. 579, 124168.

Musyoka, F.K., Strauss, P., Zhao, G., Srinivasan, R., Klik, A., 2021. Multi-step calibration approach for SWAT model using soil moisture and crop yields in a small agricultural catchment. Water 13, 2238.

Mutua, S., Ghysels, G., Anibas, C., Obando, J., Verbeiren, B., Van Griensven, A., Vaessens, A., Huysmans, M., 2020. Understanding and conceptualization of the hydrogeology and groundwater flow dynamics of the Nyando River Basin in Western Kenya. J. Hydrol.: Reg. Stud. 32, 100766 https://doi.org/10.1016/j.ejrh.2020.100766.

Neitsch, S., Arnold, J., Kiniry, J., and Williams, J. Soil & Water Assessment Tool Theoretical Documentation Version 2009, Tech. rep., 10.1016/j.scitotenv.2015.11.063, 2011.

Nkwasa, A., Chawanda, C.J., Jägermeyr, J., Van Griensven, A., 2022. Improved representation of agricultural land use and crop management for large-scale hydrological impact simulation in Africa using SWAT+. Hydrol. Earth Syst. Sci. 26, 71–89. https://doi.org/10.5194/hess-26-71-2022.

Nkwasa, A., Waha, K., Griensven, A.V., 2023. Can the cropping systems of the Nile basin be adapted to climate change? Reg. Environ. Change 23, 9. https://doi.org/10.1007/s10113-022-02008-9.

Ogega, O.M., Koske, J., Kung'u, J.B., Scoccimarro, E., Endris, H.S., Mistry, M.N., 2020. Heavy precipitation events over East Africa in a changing climate: results from CORDEX RCMs. Clim. Dyn. 55, 993–1009. https://doi.org/10.1007/s00382-020-05309-z.

Ojara, M.A., Yunsheng, L., Ongoma, V., Mumo, L., Akodi, D., Ayugi, B., Ogwang, B.A., 2021. Projected changes in East African climate and its impacts on climatic suitability of maize production areas by the mid-twenty-first century. Environ. Monit. Assess. 193, 1–24.

Olang, L.O., Kundu, P., Bauer, T., and Fürst, J. Assessing Spatio-Temporal Land Cover Changes Within the Nyando River Basin of Kenya Using Landsat Satellite Data Aided by Community Based Mapping-A Case Study, 2014.

Opere, A.O., Okello, B.N., 2011. Hydrologic analysis for river Nyando using SWAT. Hydrol. Anal. River Nyando Using SWAT 8, 1765–1797. https://doi.org/10.5194/hessd-8-1765-2011.

Ortiz-Bobea, A., Ault, T.R., Carrillo, C.M., Chambers, R.G., Lobell, D.B., 2021. Anthropogenic climate change has slowed global agricultural productivity growth. Nat. Clim. Change 11, 306–312.

Ouma, Y.O., Okuku, C.O., and Njau, E.N. Use of Artificial Neural Networks and Multiple Linear Regression Model for the Prediction of Dissolved Oxygen in Rivers: Case Study of Hydrographic Basin of River Nyando, Kenya, Complexity, 2020, 10.1155/2020/9570789, 2020.

Patz, J.A., Frumkin, H., Holloway, T., Vimont, D.J., Haines, A., 2014. Climate change: challenges and opportunities for global health. JAMA - J. Am. Med. Assoc. 312, 1565–1580. https://doi.org/10.1001/jama.2014.13186.

Peel, M.C., Finlayson, B.L., McMahon, T.A., 2007. Updated world map of the Köppen-Geiger climate classification. Hydrol. earth Syst. Sci. 11, 1633–1644.

Place, F., Njuki, J., Murithi, F., Mugo, F., 2006. Agricultural enterprise and land management in the highlands of Kenya. Strateg. Sustain. Land Manag. East Afr. Highl. 191–215.

Polley, H.W., 2002. Implications of atmospheric and climatic change for crop yield and water use efficiency. Crop Sci. 42, 131–140.

Salat, M., Swallow, B., 2018. Resource use efficiency as a climate smart approach: case of smallholder maize farmers in Nyando, Kenya. Environ. - MDPI 5, 1–15. https://doi.org/10.3390/environments5080093.

Sánchez, B., Rasmussen, A., Porter, J.R., 2014. Temperatures and the growth and development of maize and rice: a review. Glob. Change Biol. 20, 408–417.

Schaeffer, M., Baarsch, F., Adams, S., de Bruin, K., De Marez, L., Freitas, S., Hof, A., and Hare, B., Climate-change impacts, adaptation challenges and costs for Africa, Tech. rep., UNEP, Nairobi, Kenya, 2013.

Schuol, J., Abbaspour, K.C., Yang, H., Srinivasan, R., Zehnder, A.J., 2008. Modeling blue and green water availability in Africa. Water Resour. Res. 44, 1–18. https://doi.org/10.1029/2007WR006609.

Senent-Aparicio, J., Blanco-Gómez, P., López-Ballesteros, A., Jimeno-Sáez, P., Pérez-Sánchez, J., 2021. Evaluating the potential of Glofas-era5 river discharge reanalysis data for calibrating the SWAT model in the Grande San Miguel River Basin (El Salvador). Remote Sens. 13, 3299.

Shongwe, M.E., Van Oldenborgh, G.J., Van den Hurk, B., van Aalst, M., 2011. Projected changes in mean and extreme precipitation in Africa under global warming. Part II: East Africa. J. Clim. 24, 3718–3733.

Siebert, S., Burke, J., Faures, J.M., Frenken, K., Hoogeveen, J., Döll, P., Portmann, F.T., 2010. Groundwater use for irrigation - a global inventory. Hydrol. Earth Syst. Sci. 14, 1863–1880. https://doi.org/10.5194/hess-14-1863-2010.

Sinnathamby, S., Douglas-Mankin, K.R., Craige, C., 2017. Field-scale calibration of crop-yield parameters in the soil and water assessment tool (SWAT). Agric. Water Manag. 180, 61–69.

Sonkar, G., Singh, N., Mall, R., Singh, K., Gupta, A., 2019. Simulating the impacts of climate change on sugarcane in diverse Agro-climatic zones of northern India using CANEGRO-Sugarcane model. Sugar Tech. 22, 460–472.

Stockle, C.O., Williams, J.R., Rosenberg, N.J., Jones, C.A., 1992. A method for estimating the direct and climatic effects of rising atmospheric carbon dioxide on growth and yield of crops: Part I—Modification of the EPIC model for climate change analysis. Agric. Syst. 38, 225–238.

Strauch, M., Volk, M., 2013. SWAT plant growth modification for improved modeling of perennial vegetation in the tropics. Ecol. Model. 269, 98–112. https://doi.org/10.1016/j.ecolmodel.2013.08.013.

Sultan, B., Gaetani, M., 2016. Agriculture in West Africa in the twenty-first century: climate change and impacts scenarios, and potential for adaptation. Front. Plant Sci. 7, 1262.

Swallow, B.J.S., Nyabenge, M., Bondotich, D., Yatich, T., Duraiappah, A., and Yashiro, M., Tradeoffs among Ecosystem Services in the Lake Victoria Basin: ICRAF Working Paper 69. Nairobi: World Agroforestry Centre. 39 Pgs, ⟨http://www.worldagroforestry.org/downloads/Publications/PDFS/WP15658.pdf⟩, 2008.

Tatsumi, K., Yamashiki, Y., daSilva, R.V., Takara, K., Matsuoka, Y., Takahashi, K., Maruyama, K., Kawahara, N., 2011. Estimation of potential changes in cereals production under climate change scenarios. Hydrol. Process. 25, 2715–2725. https://doi.org/10.1002/hyp.8012.

Teixeira, E.I., Fischer, G., Van Velthuizen, H., Walter, C., Ewert, F., 2013. Global hot-spots of heat stress on agricultural crops due to climate change. Agric. For. Meteorol. 170, 206–215.

Teutschbein, C., Seibert, J., 2012. Bias correction of regional climate model simulations for hydrological climate-change impact studies: Review and evaluation of different methods. J. Hydrol. 456, 12–29.

Thornton, P.K., Jones, P.G., Alagarswamy, G., Andresen, J., 2009. Spatial variation of crop yield response to climate change in East Africa. Glob. Environ. Change 19, 54–65. https://doi.org/10.1016/j.gloenvcha.2008.08.005.

Tian, X., Dong, J., Jin, S., He, H., Yin, H., Chen, X., 2023. Climate Change impacts on regional agricultural irrigation water use in semi-arid environments. Agric. Water Manag. 281 https://doi.org/10.1016/j.agwat.2023.108239.

Tittonell, P., Shepherd, K.D., Vanlauwe, B., Giller, K.E., 2007. Unravelling the effects of soil and crop management on maize productivity in smallholder agricultural systems of western Kenya—An application of classification and regression tree analysis. Agric., Ecosyst. Environ. 123, 137–150.

Trisos, C.H., Adelekan, I.O., Totin, E., Ayanlade, A., Efitre, J., Gemeda, A., Kalaba, K., Lennard, C., Masao, C., Mgaya, Y., Ngaruiya, G., Olago, D., Simpson, N.P., Zakieldeen, S., 2022. Climate Change 2022: Impacts, Adaptation and Vulnerability. In: Pörtner, H.-O., Roberts, D.C., Tignor, M., Poloczanska, E.S., Mintenbeck, K., Alegría, A., Craig, M., Langsdorf, S., Löschke, S., Möller, V., Okem, A., Rama, B. (Eds.), Contribution of Working Group II to the Sixth Assessment Report of the Intergovernmental Panel on Climate Change. Cambridge University Press, Cambridge, UK and New York, NY, USA. https://doi.org/10.1017/9781009325844.011.

Tuo, Y., Duan, Z., Disse, M., Chiogna, G., 2016. Evaluation of precipitation input for SWAT modeling in Alpine catchment: A case study in the Adige river basin (Italy). Sci. Total Environ. 573, 66–82.

Velpuri, N.M., Senay, G.B., 2017. Partitioning evapotranspiration into green and blue water sources in the conterminous United States. Sci. Rep. 7, 6191.

Verdin, A., Funk, C., Peterson, P., Landsfeld, M., Tuholske, C., Grace, K., 2020. Development and validation of the CHIRTS-daily quasi-global high-resolution daily temperature data set. Sci. Data 7, 303.

Waha, K., Huth, N., Carberry, P., Wang, E., 2015. How model and input uncertainty impact maize yield simulations in West Africa. Environ. Res. Lett. 10, 024017.

Wahid, A., 2007. Physiological implications of metabolite biosynthesis for net assimilation and heat-stress tolerance of sugarcane (Saccharum officinarum) sprouts. J. Plant Res. 120, 219–228.

Waithaka, M., Nelson, G.C., Thomas, T.S., Kyotalimye, M., 2013. East African agriculture and climate change: a comprehensive analysis. Int. Food Policy Res Inst.

Washington, R. and Pearce, H., Climate Change in East African Agriculture: Recent Trends, Current Projections, Crop-climate Suitability, and Prospects for Improved Climate Model Information, Tech. rep., CGIAR Research Program on Climate Change, Agriculture and Food Security (CCAFS), Copenhagen, Denmark, ⟨www.ccafs.cgiar.org⟩, 2012.

Waswa, F., Gweyi-Onyango, J.P., Mcharo, M., et al., 2012. Contract sugarcane farming and farmers' incomes in the Lake Victoria basin, Kenya. J. Appl. Biosci. 52, 3685–3695.

Weerasinghe, I., Bastiaanssen, W., Mul, M., Jia, L., Van Griensven, A., 2020. Can we trust remote sensing evapotranspiration products over Africa. Hydrol. Earth Syst. Sci. 24, 1565–1586. https://doi.org/10.5194/hess-24-1565-2020.

Williams, J.R., Jones, C.A., Kiniry, J.R., Spanel, D.A., 1989. The epic crop growth model. Trans. Am. Soc. Agric. Eng. 32, 497–511.

Woetzel, J., Pinner, D., Samandari, H., Engel, H., McCullough, R., Melzer, T., and Boettiger, S., How will African farmers adjust to changing patterns of precipitation? McKinsey Global Institute, Chicago, USA, 2020.